Received June 23, 2020, accepted July 12, 2020, date of publication July 29, 2020, date of current version August 7, 2020.

Digital Object Identifier 10.1109/ACCESS.2020.3012662

Recent Progress in Electrical Generators for Oceanic Wave Energy Conversion

ABIDUR RAHMAN[1], OMAR FARROK[1], (Member, IEEE), MD. RABIUL ISLAM[2], (Senior Member, IEEE), AND WEI XU[3], (Senior Member, IEEE)

[1]Department of Electrical and Electronic Engineering, Ahsanullah University of Science and Technology, Dhaka 1208, Bangladesh
[2]School of Electrical Computer and Telecommunications Engineering, University of Wollongong, Wollongong, NSW 2522, Australia
[3]State Key Laboratory of Advanced Electromagnetic Engineering and Technology, School of Electrical and Electronic Engineering, Huazhong University of Science and Technology, Wuhan 430074, China

Corresponding author: Wei Xu (weixu@hust.edu.cn)

This work was supported in part by the National Natural Science Foundation of China under Grant 51877093.

ABSTRACT Oceanic wave energy extraction through electrical generator is one of the most interesting topics in the field of power engineering. Almost all the existing relevant review paper focus on electrical generator with the working principle of electromagnetic induction or piezoelectric or triboelectric effect. In this paper, all the existing types (based on principle of operation) of electrical generator used for wave power harvesting are discussed. This paper not only covers recent progress in electrical power generation by electro-magnetic induction, piezoelectric generator, and electrostatic induction, but also presents critical comparative review as well where suitable use and weakness of each type of generators are discussed. Moreover, the application of advanced magnetic core, winding, and permanent magnets are discussed with extensive explanation which are not focused in the existing reviews. Various new constructional features of the electrical generators such as split translator flux switching, two-point absorber, triangular coil, dual port linear generator, piezoelectric, triboelectric nanogenerator, etc. are highlighted with principles of operation. It also includes emerging human intervened optimization method for determining optimum shape of generator and cooling system which is necessary to prevent demagnetization of the permanent magnet. Finally, the way of supply the generated electrical power form the generator to load/grid is thoroughly described in a separate section that would be obvious for successful operation. The comparison among all types of generators in terms of output voltage, current, scale of power production, power-frequency characteristics, power density, cascading, and approaches are tabulated in this paper.

INDEX TERMS Electrostatic induction generator, linear electrical generator, magnetic material, optimization, permanent magnet, piezoelectric generator, superconductor, wave energy converter.

NOMENCLATURE

DPLG	Dual port linear generator
EFHAS	Elastic floating unit with hanging structure
EMG	Electromagnetic generators
FPED	Flexible piezoelectric device
HF-10	DI MAX HF-10
HF-10X	DI MAX HF-10X
HF-12	DI MAX HF-12
HIGA	Human intervened genetic algorithm
HTS	High temperature superconductors
LG	Linear generator
M-27	DI MAX M-27
NdFeB	Neodymium iron boron
OWE	Oceanic wave energy
PMLG	Permanent magnet linear generator
RES	Renewable energy source
TENG	Triboelectric nanogenerator
WEC	Wave energy converters
YBCO	Yttrium barium copper oxide

The associate editor coordinating the review of this manuscript and approving it for publication was Michele Magno.

I. INTRODUCTION

With technological advancements and increasing human population, the demand for electrical energy is growing precipitously. To facilitate the demand of electricity at global scale, the electrical power generating capacity must be increased. At present, most electrical generators rely greatly on fossil fuels. It is a fact that fossil fuels such as coal, petroleum,

and gasoline are non-renewable energy sources and are diminishing at a rapid rate. These sources emit carbon dioxide and other greenhouse gases which are detrimental to the nature. Forecasted results demonstrate that by the end of this century the average temperature of the earth surface would rise by 1.4–5.8°C. Moreover, the warming rate is expected to be 0.02°C per annum based on recent decades [1]. The consequences caused by carbon emissions will primarily be observed near the coastal areas due to the rise of sea water level. Moreover, small islands may completely be flooded if this issue is not addressed. Scientists and researchers have investigated for many years to find a replacement of fossil fuels to lessen the impact on environment. Renewable energy source (RES) such as solar, wind, hydropower, biomass, and geothermal are used as an alternative to conventional fuels since they are widely available and cause little to no harm to nature.

The total power generating capacity of different RESs are presented in Fig. 1 [2]. RESs such as hydro, wind, and solar have the highest capacity compared to others as vast research is conducted in these fields since many years. Extensive research on solar, wind, and hydropower enables us to harness large amount of energy through these. On the other hand, oceanic wave energy (OWE) retains considerable amount of energy yet its installed capacity is infinitesimal as compared to other RESs.

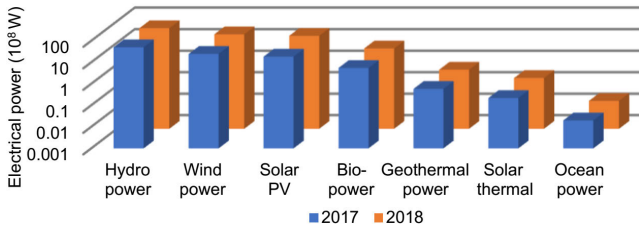

FIGURE 1. Electrical power generated from various RESs.

Many RESs such as wind and solar has large installed capacity but are intermittent in nature. Generation through wind energy relies on the availability and direction of wind speed. As for solar energy, solar radiation is required which depends on diurnal period and weather condition. Hence, sophisticated energy storage device is essential to mitigate the issue of power discontinuity. There are other RESs such as geothermal and hydropower plants which can only be implemented in few areas throughout the world because of their lack of availability. On the other hand, OWE is readily available in the ocean and it is not site specific which makes it a desirable preference over many other RESs. Moreover, the energy density of OWE is commendable.

Electricity generation through OWE was first proposed in the late 18th century. OWE has been considering one of the potential RESs in many countries since 1973, due to the oil crisis. Around 1–10TW of electrical power can be extracted from oceanic waves which could serve a significant amount of the world's electrical power demand. Wave energy greatly depends on different factors such as magnitude, frequency, wavelength, distance from the shorelines etc. Given the location of oceanic waves such as near shore, offshore or shorelines, approximately 50–100kW power per meter of wave front could be generated [3].

UK, US, Japan, India, Australia and many other countries have adopted the OWE converters to serve their energy demand [4]. EU aims to fulfill all its energy demand through RESs out of which approximately 0.02% of energy is currently delivered by OWE. The leading nation, focusing on OWE, UK aims to fulfill 20% of their total demand from OWE by 2020. Ireland has set a goal to produce 0.5GW power through OWE by 2020 [5]. In Scotland, a wave energy project is installed which can produce 150kW of power [6]. The expected wave power in Europe is approximately 20–60kW/m. Around 1170TWh/year of energy can be harvested from OWE [7]. The nearshore OWE of China is nearly 249.7TWh/year [8]. Approximately 50TWh/year of OWE is acquired by UK [9].

Oceanic wave creates mechanical movement in wave energy harvesting devices. Waves are random in nature that affects wave energy devices. These devices are namely Wave Dragon, Pelamis, Limpet, Archimedes wave swing, etc. The random mechanical movements are not rotational. However, with the aid of auxiliary devices, the random motion can be converted into stable rotational movement. But considering the monetary cost, energy loss, and complex maintenance, the auxiliary devices are subjected to further assessment. Hence traditional devices are not suitable to harvest wave energies. Special type of device along with generator are required to convert the mechanical movements into electrical energy. Majority of these generators are linear generators (LGs) operated by the principle of electromagnetic induction. Recently, small scale piezoelectric and triboelectric generators are tested for this purpose. Energy extraction from OWE is still at its initial stage and extensive research is required to become fruitful as wind and solar power plants.

Floating point observes are modeled in [10] through numerical methods, such as empirical method, Navier-Stokes equation, and boundary integral equation. However, the review does not discuss about connecting these generators with the grid. Moreover, other types of wave energy converter are not modeled. In [2], different wave energy conversion techniques are introduced for electromagnetic and piezoelectric generators. Moreover, the review also discusses about different wave energy converters such as point absorber, overtopping device, oscillating water column. Finally, various control scheme is shown to regulate the output from these devices. Nevertheless, triboelectric generators are not considered in the review. Moreover, sustainable operating environment for different type of generator is not explained. Recent improvement in the field of piezoelectric material-based energy harvester is discussed in [11]. Energy harvesting characteristics of different types of piezoelectric devices are illustrated. Various electronic circuits required to operate the piezoelectric devices are showed in this review.

However, no discussion has been made on other type of wave energy harvesters such as electromagnetic generators or triboelectric nanogenerators. Moreover, these reviews do not provide adequate guidelines for grid connectivity with the generators.

Electrostatic generators can be considered useful for harnessing energy from ocean, especially for low frequency waves. Current progress of this technology is reviewed in [12] where various types of energy harvesting devices with electrostatic generators are presented. However, detailed analysis of suitable operating condition is not described. Application of advanced material for different electrical generator is not presented. The review mentioned the necessity of grid connection, but not presented at all and left in the future scope.

However, to the best of authors' knowledge, no review is found that delineates on the recent development of electrical generators, their critical review, and aggregation or grid connection for oceanic wave energy extraction together. In this context, this paper presents recent development of almost all types of electrical generators incorporating electromagnetic, piezoelectric, and triboelectric generators. The structure of different types of wave energy converters are expounded. Additionally, use of advanced materials in these generators and their effects are explained. Structural improvement, shape optimization of LGs, and connection between wave energy converters with the grid are discussed as well. Organization of this paper is as follows.

Section two discusses about various linear generator. Section three focuses on recent progress in power capturing method from the oceanic wave. The subsequent section illustrates recent structural progress in LG. The application of superconducting windings is discussed in section five. Advanced permanent magnets used in linear generator are described in section six. Various types of magnetic cores are illustrated in the subsequent section. Section eight shows piezoelectric material based electrical generators. Electrostatic induction based electrical generators are presented in the following section. The scheme of transferring generated power from oceanic wave to load/grid is explained in section ten. Finally, a brief discussion and conclusion are included.

II. LINEAR ELECTRICAL GENERATOR

The linear generator is now the center of attention of oceanic wave energy conversion as it directly converts mechanical energy into electrical energy in bulk amount. The mechanical energy is obtained from translational motion through wave energy devices. Most of the linear generator consists permanent magnet, but there are several classifications depending on construction, working principle, and physical shape.

A. CONSTRUCTION

LG mainly consists of active materials such as magnetic core, winding, and permanent magnet as required in rotating generator. Depending on construction or architecture, LG can be tubular, flat, or complex structure which are described in the following.

1) TUBULAR LINEAR GENERATOR

Construction of a tubular linear generator is similar to the flat linear generator. Both generators contain a stationary stator and a moving translator. Generally, cross sectional views of the stator and translator of a tubular generator is circular. A tubular structured LG having permanent magnet placed on the primary side is designed in [13]. The moving part i.e. the primary side is linked with the buoy and the stator part i.e. the secondary side is fixed. Both windings and permanent magnets are placed in the primary side. Ferrite core is used in the stator side although any type of core can be used. Higher output frequency is observed from the prototype of this generator. To validate the findings, the proposed generator is compared with a tubular LG which has its permanent magnet placed on the secondary side. The comparison results show that efficiency of the proposed generator is higher [13]. In addition to that, the electromagnetic resistance ripple is also lower. Moreover, the detent force is reduced while having a simple structure. Detent force is the cause of creating mechanical vibration which is needed to be avoided.

2) FLAT LINEAR GENERATOR

Cross sectional view of flat liner generator is mostly rectangular. Flat linear generator can be single sided, double sided or four sided as well. Its construction is simpler compared to tubular one. Both tubular and flat linear generator have their own advantages and disadvantages. The magnetic flux distribution in a tubular linear generator is more even compared to the flat one. On the other hand, tubular generators are difficult to disassemble compared to a flat linear generator.

3) OCTAGONAL LINEAR GENERATOR

Octagonal linear generator is complex in architecture and not a common type linear generator. A 100kW rated linear generator for oceanic wave energy conversion is proposed in [14] in which cross sectional shape of the stator is octagonal. The primary focus of this study is to reduce the voltage harmonics and power fluctuation which would result in reduced cogging force. If the cogging force is not maintained, it disturbs the piston movement and creates uneven airgap. The quantity of slots for each pole and phase is varied to obtain the desired results. For the decreased power fluctuation, the voltage waveform closely resembles pure sinusoidal waveform. Furthermore, for the smooth pole, the fluctuation also decreases under the condition of increased load angle. Though the proposed LG decreases the power fluctuation, its construction is quite complicated to implement.

B. WORKING PRINCIPLE

According to working principle, linear generators can be mainly classified as permanent magnet, switched reluctance, flux switching, and induction. Each type of linear generator, such as flat or tubular, can be operated by any of these working principles. Permanent magnet linear generator (PMLG) can be synchronous or asynchronous. Switched reluctance

machine does not contain permanent magnet. Generally, linear induction generator is not found for wave energy extraction. Almost all the linear induction machines are used as motors because it is not suitable to be used as generators for this purpose. Among all these types of LGs, PMLGs are mostly found because of its high-power density.

1) PERMANENT MAGNET LINEAR GENERATOR

PMLGs are prominent over the other types because of its ability to generate high amount of electrical power. PMLG can also be tubular, flat as shown in Fig. 2(a), octagonal or it can have any other special construction. Most of the flux switching linear generator are in the category of PMLG.

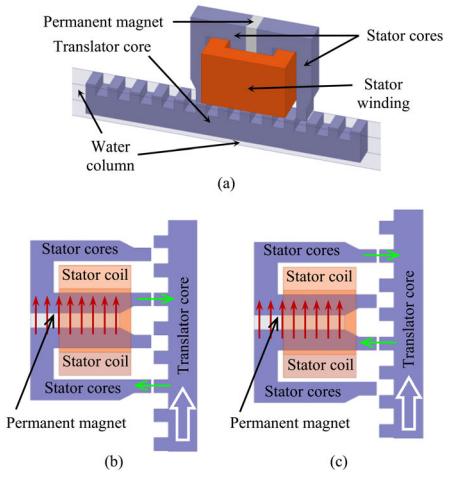

FIGURE 2. A flux switching permanent magnet LG: (a) isometric view, (b) time t_1 and (c) time t_2.

2) SWITCHED RELUCTANCE LINEAR GENERATOR

Switched reluctance generator does not have a complex structure, but its control is difficult. A controller is developed in [15] for a switched reluctance LG to control the voltage ripple and also to reduce the error associated with the drive circuit. A current distribution function using the principle of minimized copper loss is developed to decrease the ripples associated with phase current. It is demonstrated that the voltage ripples are limited within approximately ± 0.5V with reduced error.

3) FLUX SWITCHING LINEAR GENERATOR

Flux switching LG works on the principle of magnetic flux switching in the stator core (in general) for which there is a rate of change in magnetic flux around the stator winding. A typical flux switching PMLG has two parts as illustrated in Fig. 2(a). The translator connected with the buoy moves vertically as the oceanic waves tend to create vertical displacement on the buoy.

The stator consists permanent magnet and copper coil. During time t_1, if the wave elevates the buoy, the translator moves and the direction of net flux Φ_g corresponds to the direction of Fig. 2(b). The direction of magnetic flux is shown by arrow. For the period of t_2, the buoy moves again for which the flux line changes its direction that corresponds to Fig. 2(c). The operation can be even simply understood by following the stator and translator tooth alignment.

This section briefly summarizes various types of LG with different shapes. From the observation, most remarkable LGs are tubular and flat. On the other hand, LGs are also classified based on their working principle such as, PMLG, switched reluctance LG, and flux switching LG are noteworthy.

III. RECENT PROGRESS IN POWER CAPTURING METHOD FROM THE OCEANIC WAVE

Electrical power generation from the oceanic wave can be increased by either improvement of generator or increase the power capturing capacity as described in the following.

A. TWO-POINT ABSORBER

Traditionally, the absorption process of oceanic wave energy is conducted by using a single point absorber. In this method, a single buoy is used which can either be floating or submerged. The linear generator is connected with the absorber. To make the absorption of energy more efficient, a resonant two body system wave energy converter is proposed in [16] in which a surface buoy and a passive buoy is integrated. The surface buoy floats while the passive buoy creates inertia for damping. This combination helps the buoy to follow the wave frequencies more closely. The hydrodynamic characteristics of the proposed device is investigated through time domain and frequency domain analysis. In irregular waves, the power capture ratio of the converter is approximately 80%. Moreover, the coupling between LG, passive buoy, and surface buoy became rigid when a translator of 14 ton is used. Furthermore, around 80% of power capture ratio is achieved by placing the passive buoy at a depth of 40m. However, if the depth is decreased by 30m then the power capture ratio becomes 50%. Additionally, the power spectrum for different frequencies of the wave are showed. At nearly 1.2rad/s, the power spectrum is concentrated. Thus, a narrow power spectrum would be efficacious for resonance behavior of two body system linear generators.

B. NARROW TEETH AT BOTH ENDS

In [17], it is shown that the conventional permanent magnet linear generator is unable to produce power for 2–3 seconds due to unavailability of vertical velocity of the translator at the top and bottom position. To mitigate this effect, the shape of the translator teeth and stator teeth is made narrow at its two ends. Hence, the number of teeth increased at the two sides. As a result, the power discontinuation of the PMLG decreases noticeably. Moreover, the ripple and output power of the proposed PMLG is compared with the conventional one. The results show that the proposed PMLG performs better than the conventional PMLG. Additionally, if the length of the translator is increased than the stator, then the performance increases as well.

C. IMPLEMENTATION OF DUAL PORT METHODOLOGY

Most of the available LGs use only a single port for mechanical power transfer and another port for electrical power transfer. Since the conventional single port LGs provide a discontinuous supply of power from the oceanic wave energy, a dual port linear generator (DPLG) is required for continuous supply.

To address the problem associated with power discontinuation, a novel DPLG is proposed in [18] which has two translators. The top positioned translator is called driver translator whereas the other is referred as driven translator. These two translators are enclosed by a cage. The buoy is directly connected with the driver translator and the driven translator is connected to the driver translator with a spring. Both the translators are connected to the cage by damping springs to avoid direct contact. Fig. 3(a) shows the construction of the proposed DPLG. Furthermore, a prototype of the proposed generator is constructed in a laboratory as depicted in Fig. 3(b) for validation of the results.

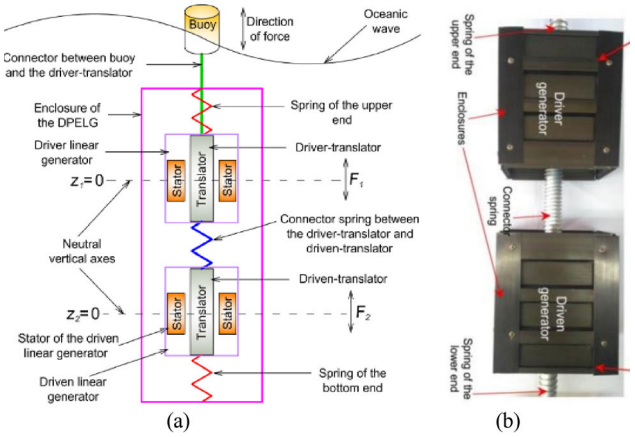

FIGURE 3. Dual Port LG: (a) proposed model and (b) downscale prototype [18].

Fig. 4(a) shows the vertical velocity of the two translators under fixed angular velocity, ω. When the driver translator does not have velocity, the driven translator shows maximum velocity.

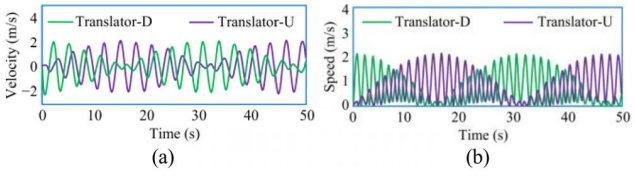

FIGURE 4. Characteristics of the driver and driven translator: (a) velocity and (b) speed.

At this time, electrical power can be generated from the driver translator whereas no significant amount of power can be delivered by the driver translator. Also, when the driven translator experiences zero velocity, the driver translator exhibits its maximum velocity. In this case, the driven translator shows inadequate power supply and the driver translator generates power. The speed which is generated from the two translators are shown in Fig. 4(b).

The driver and driven generators are clearly identified in the equivalent circuit of the proposed dual port linear generator which are connected in series with the winding resistance. The generators' output is fed to a rectifier followed by a filter. Finally, a resistive load is connected to simulate the performance of the DPLG. The design of stator tooth must be handled carefully as it effects the performance and efficiency of the DPLG. Therefore, the stator tooth slope and curvature are optimized using genetic algorithm.

The experimental and simulated results are shown in Fig. 5 where it is observed that, power is being generated by the driver generator while the driven generator does not have any vertical velocity. Quite the opposite, when driver generator has no velocity, the driven generator produces power. Moreover, the waveforms are remarkably similar to each other.

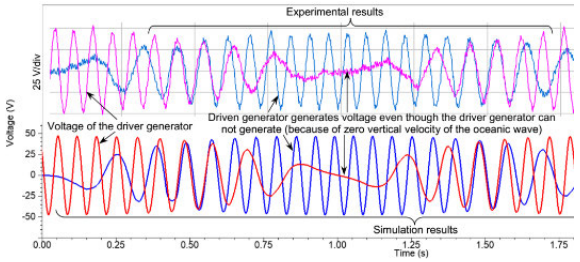

FIGURE 5. Experimental and simulation results of generated voltage.

Techniques to capture power from the oceanic wave is discussed in this section. It is found that, recent advancement includes adoption of the two-point absorber, using narrow teeth at two ends of the translator, and utilization of dual port methodology.

IV. RECENT STRUCTURAL PROGRESS IN LG

Although LG is associated with various construction and working principle, few common limitations are found regardless of their classifications. These are problem with translator weight and optimization in shape of the LG. This section covers the structural advancement as addressed in the following.

A. MINIMIZATION OF TRANSLATOR WEIGHT

Study shows that the translators are usually solid and heavy due to their rugged structure. Thus, the vertical motion of the translator gets slowed down. Mathematical relationships between the mass of the translator and its acceleration are demonstrated in [19] which are

$$\frac{d}{dt}(z_{tr}) = v_{tr}, \frac{d}{dt}(v_{tr}) = a_{tr} \tag{1}$$

$$a_{tr} = \frac{\rho g \pi a^2 [z_{tr} - Z_w(t)] + (R_r + R_v)[v_{tr} - v_w(t)]}{M_b + M_w + M_{tr}} \tag{2}$$

where the relation between vertical displacement z_{tr}, velocity v_{tr}, and acceleration a_{tr} of the translator is described. On the other hand (2) demonstrates the equation of acceleration where, ρ denotes the mass density of sea water, R_r is the radiation resistance, g is gravitational acceleration, R_v is viscous resistance of ocean water, M_{tr} is the mass of floating buoy, and M_w the added mass due to sea water. From hydrodynamic analysis, the value of R_r and R_v are acquired. From these equations, it can be comprehended that, the mass of the translator is at the denominator of (2). Hence, reducing the translator mass significantly increases the acceleration. The induced voltage, $v_i(t)$ is found by Faraday's law of electromagnetic induction as

$$v_i(t) = -N_c \frac{d\overline{\Phi}}{dt} \tag{3}$$

where N_c is the turn number of winding and Φ is the magnetic flux. As vertical displacement of the oceanic wave is similar to sine function, the flux can be expressed as

$$\Phi(t) = \overline{\Phi} \sin\left(\frac{2\pi}{\lambda} z(t) \pm \underset{j}{\theta}\right) \tag{4}$$

where $2\pi/\lambda$ and θ_j represent total number of magnetic pole pairs in an oceanic wave cycle and initial phase angle, respectively. Combining (3) and (4), voltage of the linear generator can be expressed as follows

$$v_i(t) = \overline{V}_p cos\left(\frac{2\pi}{T} t\right) cos\left\{\frac{\pi z_{p-p}}{\lambda} sin\left(\frac{2\pi}{T} t\right)\right\} \tag{5}$$

where V_p is the peak voltage and z_{p-p} is the peak to peak vertical displacement. Although the sea wave is sinusoidal in nature, the size of the buoy is infinitesimal compared to the size of the sea wave. Therefore, it is considered in [19] that the buoy experiences the wave as plain surface. This approximation is done to simplify the dynamic mathematical model of oceanic wave. Moreover, Fig. 6 demonstrates a rainbow spectrum showing the magnetic flux density, B of a traditional flux switching permanent magnet linear generator.

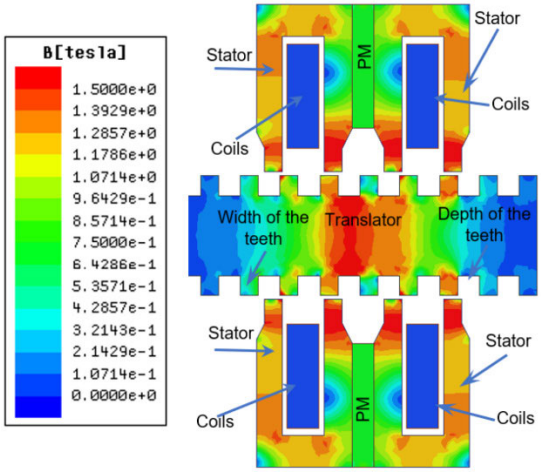

FIGURE 6. Distribution of magnetic flux density in the linear generator.

For a certain position in the translator, the magnetic flux density reaches its maximum value (red color). However, there are some portions of the translator where the value of B becomes significantly lower (blue color). Hence, minimization of those areas of the translator is possible which eventually reduces mass of the translator.

To address these concerns, a novel idea is developed in [20] where the translator is split vertically into two sections as shown in Fig. 7. The split translator is placed between the main stator and an additional supporting stator. The size of the supporting stator is chosen in such a manner that it supports the translator to pass all the flux and accommodates the area where the maximum flux density occurs. The trapezoidal shape of the supporting stator creates hollow spaces which is covered by nonmagnetic material in [19] as denoted by "NMM". This new generator having two 7.5mm thick translators and the traditional 24mm translator can generate equal amount of power. The translator retains half the amount of mass of a conventional translator thus achieving 13.185% increase of efficiency. Although flat type flux switching LG is used for explanation, this method is also applicable for tubular LG.

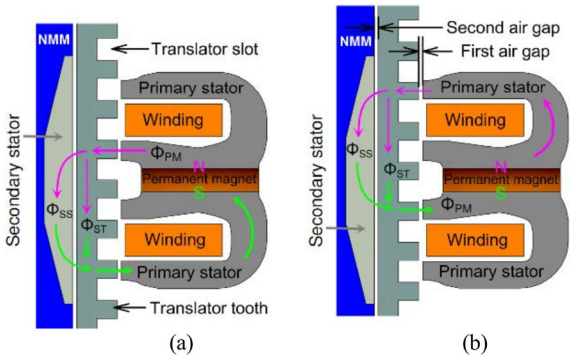

FIGURE 7. Cross sectional view of a split translator supporting stator linear generator [19].

B. SHAPE OPTIMIZATION OF LINEAR GENERATOR

Shape optimization is introduced in [21], that enhances electrical power generation dramatically despite of using less amount of active material in the LG. Several studies are carried out on linear generators using genetic algorithm where the parameters such as length, pole-tooth gap, depth, air-gap length, and pitch are deemed. Most of the traditional genetic algorithms do not utilize the human capability/involvement for optimization approach. Thus, human intervened genetic algorithm (HIGA) is used in [21] to optimize the shape of the LG. The algorithm on a flux switching permanent magnet linear generator is simulated. The proposed algorithm can quickly determine better design that can harvest more power than existing schemes with reduced number of generations. Bezier curve is used to describe the shape of stator and translator teeth. In the beginning of the process, four different shapes of stators and translators are considered as initial population. Afterwards, the output powers of these shapes were

observed to identify the best structure and the stator-translator combination. The stators having curved edges have performed better than their sharped edged counterparts. After 4 generations, two translators with the highest fitness values were selected. Then the performance of the proposed structure with and without applying HIGA are compared to the same linear generator. The shape of the proposed structure significantly reduces the reluctance as well as leakage flux than the structure without applying HIGA. Moreover, the flux density (in both stator and translator) is also appreciably higher in the proposed structure. Even though there is not much change in eddy current between the two structures, the reduction of hysteresis loss is appreciable. Furthermore, the voltage and flux linkage between the two structures show that the proposed structure outperforms. It experiences less applied force under same loading conditions. The importance of selecting proper Bezier curve is emphasized for developing the linear generator. Another structure with an improper and trivial selection of Bezier curve demonstrates that a considerable amount of flux density is reduced throughout the structure. By adopting HIGA, the power is increased by 26.6% while the size of the machine is reduced by 14.19%.

Moreover, the flux intensity, density, and lines for both optimized and un-optimized stator tooth are shown where more flux linkage for optimized stator teeth is observed. The optimized values of inductance and capacitance of the filter for which under-, over-, and critically damped voltage is observed and overshoot is minimized. The electrical parameters and the final optimized stator tooth are also shown in [18]. The optimized curvature is approximated by a polynomial.

The force ripples are effectively minimized in the proposed dual port linear generator while considering without optimization, slope optimization, and slope-curvature optimization. Furthermore, the core loss for both with and without optimization of stator teeth are also shown where the core loss is reduced in the optimized design. Additionally, the hysteresis loss and eddy current losses are also decreased accordingly. It is mentioned that the proposed dual port linear generator with slope and curve optimization has reduced the force ripples by approximately 40.98% and the generated power is increased by approximately 17.98W.

It is found from this discussion that, optimization of the shape has been introduced very recently to enhance the performance of LG. Moreover, to obtain better power output by improved dynamics, weight of the LG is also minimized.

V. SUPERCONDUCTING LINEAR GENERATOR

The electrical power extraction from the traditional generator is inadequate because of armature resistance. Since there is no internal resistance in superconductor, copper loss can be minimized by replacing copper conductor with it. As such, the overall power loss reduces and hence the power output increases. Based on the critical temperature, which is required to maintain superconductivity, superconductors are classified into two categories. One is low temperature superconductor which demonstrates zero internal resistance at extremely low temperature. It requires expensive liquid helium to maintain this temperature. The other is high temperature superconductor (HTS) which can be operated at relatively higher temperature and can easily be maintained by low cost liquid nitrogen. Most of the HTS are copper oxides and are often referred as cuprates. The first generation of superconductor is used in industries due to its multifilamentary tape-based structure. As for the second generation of superconductor, it has coated tape-based structure. Moreover, its main attributes are enhanced current density, greater tensile strength, and improved consistency. Furthermore, if superconductors are utilized then it will reduce the slot size of the winding compared to copper winding provided that ratings of other parameters are equal. The reason for this is due to higher current rating and zero internal resistance of superconductor. Reduction in slot size will eventually decrease size of the linear generator. Also, the output power will be enhanced for avoiding copper loss. Hence, for the same amount of power, the generator size can be significantly reduced which in turn reduces the cost and improve its usefulness.

Two models of superconducting linear synchronous generators are proposed in [22]. The secondary mover has either tape coil or bulk magnet array both of which is made of HTS. The HTS bulk magnet is the replacement of conventional permanent magnets whereas the HTS coils are the replacement of conventional copper coil. Yttrium barium copper oxide, a high temperature superconductor, is used for the bulk magnet and Ansoft/Maxwell is used for simulation.

For the translator velocity (of this generator) 3m/s and the airgap 2mm, B is increased from 2T to 4T. It results in no load RMS voltage 28.9V for 2T and 108.9V for 4T. For 8mm and 2mm air gap length, the no-load RMS voltages are 71.4V and 108.6V, respectively at $B = 3$T. Similar approaches were made to HTS coil type generator except that excitation current is varied as well. For the change in excitation current from100A to 200A, the no-load RMS voltage increases from 76.4V to 123.9V.

It is commonly found that decrease in air gap or increase any one of flux density, velocity, and excitation current enhances the voltage and power in the HTS linear generators. Another superconducting LG is proposed in [23] where permanent magnets are placed in the stator. Simulation results are presented for voltage, current, power, and applied force. It is considered that the applied force is approximately 150N and the velocity for the translator is 1m/s. The output power is the product of applied force and velocity. From simulation results, it is seen that the output power is close to 150W. It is also shown that, if the air gap is changed, the current and voltage also changes. The current is maximum for 1mm of airgap as it is the minimum air gap length. Furthermore, the output voltage is roughly a square wave which requires less filter to rectify.

Effect of load variation is also presented in [23] where the current and power drops significantly and terminal voltage increases when load is decreased beyond 3Ω. For this reason, 3Ω is selected as operating point. From force, power and

efficiency plots it is found that the power is maximum at 2Ω, but the efficiency and force are too low. Efficiency of the proposed generator is 96% for 10Ω load resistance provided that the frictional and other mechanical losses are neglected. The core loss of the generator is only 0.3% which creates negligible amount of heat. Since the superconducting property of superconductors are likely to deteriorate beyond cryogenic liquid temperature, the proposed generator is highly suitable to incorporate superconductors.

Second generation HTS tape-based superconductor is used in [24] which has an average thickness of 0.1mm and width of 4mm. Fig. 8 illustrates the magnetic property of the proposed superconductor based LG.

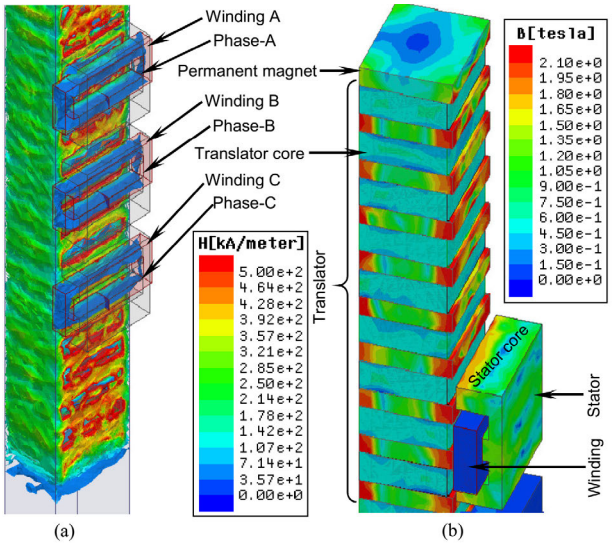

FIGURE 8. The superconducting LG: (a) magnetic field intensity and (b) flux density [24].

Moreover, its critical current rating is 400A and critical temperature is 77K. Furthermore, it has a tensile strength of 500MPa. Fig. 9 shows the voltage and power waveform of a linear generator having superconducting and ordinary copper wire.

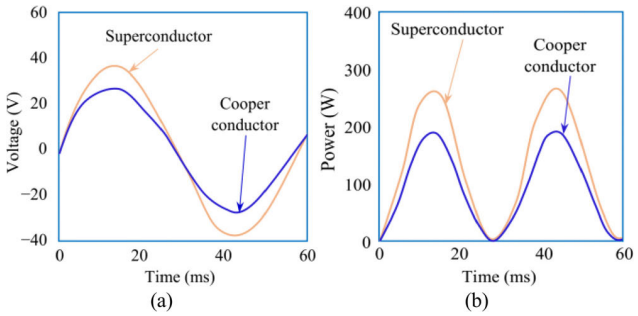

FIGURE 9. Comparison of (a) voltage and (b) power output.

Generator made of superconductor provides better terminal voltage and power output than that of using copper. To maintain the characteristics of the superconductor, it is essential to minimize the temperature which is produced in the generator. One of the main sources of heat is core loss which can be minimize by applying advanced magnetic core. The combination of DI MAX HF-10 (called HF-10 herein after) based core and yttrium barium copper oxide (YBCO) based superconductor performs better than other combinations as shown in [24]. The power and core loss of steel, DI MAX M-27 (called M-27 herein after), and HF-10 magnetic cores under high temperature superconductor based linear generator are also tabulated. It is observed that, HF-10 core outperforms the other two by having less core loss and more output power. The usual iron core demonstrates 6% core loss when it generates 302.1W power. Whereas M-27, a non-oriented iron core, exhibits 331.3W output power with 2.65% core loss. For HF-10, core loss is minimized to 2.4% with approximately 23W additional output power compared to that of conventional one.

A superconductor-based generator is proposed in [25] where the stator is made of neodymium iron boron (NdFeB) permanent magnet and the translator has laminated ferromagnetic core. The generator results more terminal voltage and produces additional 30% electrical power than that of the traditional one. YBCO is used for the winding of this generator. Finite element technique through ANSYS/Maxwell simulation software is used to demonstrate its performance. The performances of the proposed and traditional generator are compared where the proposed one demonstrates excellent performance. Table 1 identifies the consequence in the LG for using ordinary copper conductor and superconductor-based winding.

TABLE 1. Outcome of the LG using copper conductor and superconductor based winding.

Winding	Type of Generator	Outcome
Copper	PMLG (stator or translator)	➢ High power loss due to internal resistance ➢ Low winding factor
YBCO HTS	Flux switching PMLG	➢ Higher output power ➢ Terminal voltage increased [25]
YBCO HTS	Linear synchronous generator	➢ Voltage and power increased [22]
2G tape-based superconductor	HTS LG	➢ Higher terminal voltage than copper ➢ Output power increases [24]

This section shows the important features of HTS based winding to be used in the superconducting LGs. HTS tapes are suitable for constructing coils or armature winding in the PMLG. It is also suitable for designing a superconducting magnetic LG. With the HTS based PMLG, it is expected that, much higher output power can be achieved in near future.

VI. SPECIAL PERMANENT MAGNETS IN LG

Most of the existing permanent magnet linear generator incorporates conventional NdFeB permanent magnets. These permanent magnets tend to demagnetize when the temperature of the generator increases. Thus, the power generation decreases eventually. The following sub-sections describes the way of preventing demagnetization, thus producing high power.

A. APPLICATION OF HIGH-GRADE PM

High graded permanent magnets can retain its remanence magnetism even at high amount of reverse magnetic field. A PMLG with high graded N48H NdFeB is proposed in [26] to maintain adequate amount of remanence in it. Temperature effect on demagnetization is illustrated in Fig. 10. Fig. 10(a) shows the comparison of demagnetization curve between conventional N35 and proposed N48H under 60°C temperature. N48H outperforms N35 in terms of magnetic flux density and coercive field strength under the same temperature. The proposed generator is simulated using ANSYS/Maxwell. Finite element analysis is used to demonstrate the results. The voltage, current, and power comparison show that the N48H performs better in all these aspects. Additionally, the core loss for using N48H is lower than that of using N35 for the same power and the generator with N48H delivers 44W more power than that for using N35. Around 28% increase in electrical power is achieved by integrating N48H instead of using conventional N35 for the same design and other parameters.

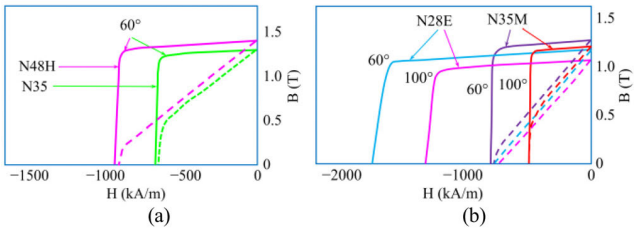

FIGURE 10. Characteristics curves of (a) N48H and N35 at 60°; (b) N35M and N28EH at 60° and 100°.

Another high graded N28EH material for permanent magnet is used in [27] and the results are compared with conventional N35M PM. Fig. 10(b) depicts the magnetizing curve for both of the materials. It is observed that the performance of N28EH is better than using N35M at both 60°C and 100°C. Fig. 11 shows that at low temperature, usual N35M graded permanent magnet can generate enough power but it degrades at high temperature. This is due to reduced residual magnetism.

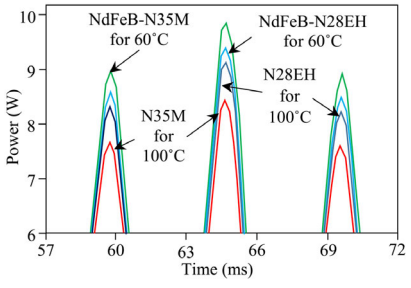

FIGURE 11. Instantaneous power at 60° and 100°.

But, for selecting N28EH, the LG can generate more power than that of using the other. Demagnetizing curves of N52, N38, and NdFeB is plotted in Fig. 12. Outcome of N52 is

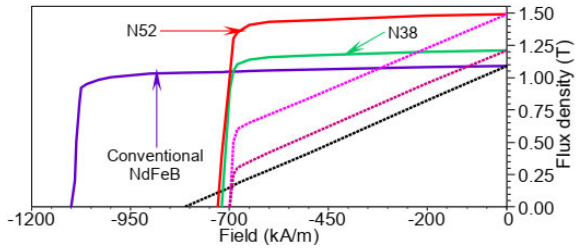

FIGURE 12. Demagnetizing curves of conventional, NdFeB, N38, and N52.

better than the other two materials. Therefore, using N52 with Supermendur generates the highest electrical output power than any combination formed by other materials.

B. APPLICATION OF HALBACH ARRAY

Halbach array is the special arrangement of permanent magnets that results increase in magnetic field in a particular direction. Quasi-Halbach magnetization structure is presented in [28] where a tubular permanent magnet linear generator with a bulged stator and auxiliary slots is used to reduce the detent force. The detent force of a conventional 8 pole 12 slots PMLG is compared with the proposed 9 pole 10 slots PMLG. It is demonstrated that the proposed generator has reduced the detent force by 82.56%. Furthermore, with the help of finite element analysis and Fourier transformation, it is demonstrated that changing the length of the bulged stator significantly reduces detent force. Through parametrization analysis, size of the bulged stator is optimized. For the size of 3mm, the detent force reduces from 159.72N to 20.47N which is a reduction of around 87.18%. Additionally, the relation of voltage and airgap is analyzed where it is demonstrated that 1mm of airgap can results more voltage than that of using 3mm of airgap. However, for manufacturing ease, it is suggested to use 3mm of airgap.

An external tubular PMLG is demonstrated in [29] where quasi-Halbach array is used to maximize the airgap flux density. Moreover, auxiliary frictional slots and assistant teeth are incorporated to reduce detent force. The cogging forces are compared with and without auxiliary slots. When the width of the auxiliary slots is adjusted to 8mm, detent force is reduced by approximately 68.98%. At 18Ω loading condition, the power density increases by 7–8 times with an efficiency of 90.03%. Moreover, a prototype is built to compare the simulation results with the experimental one.

C. PREVENTION OF DEMAGNETIZATION

Demagnetization or degradation of the remanence magnetism often occurs in the LG while producing electrical power. It can be minimized by either using high graded permanent magnets, maintaining low temperature, or avoiding permanent magnets. High graded permanent magnet which is used in the LG for preventing demagnetization is costly. Hence, to prevent demagnetization, temperature control could be one of the effective methods for the PMLG.

1) ELECTROMAGNETIC AND SUPERCONDUCTING LG

A novel electromagnetic linear generator is proposed in [30] which is almost solve the demagnetizing problem. The LG uses a permanent magnet excitation generator to excite other electromagnetic LGs. Moreover, m-shaped poles and pole shifting technique are used to reduce the amount of leakage flux, force ripples, and cogging forces. ANSYS/Ansoft is used for performance evaluation. However, the excitation generator consumes 25% of the total generated power.

2) TEMPERATURE MINIMIZATION IN THE PMLG

A cooling system which can reduce the rising temperature of the generator is proposed in [31]. The cooling system contains a control unit, a chiller, a dehumidifier-based air handling unit, water pipes to circulate the chilled water. Fig. 13 shows the block diagram of the chiller embedded in PMLG. The model demonstrates better performance regarding terminal voltage, current, and generated power. It is demonstrated that the proposed cooling system based PMLG provides 2.2kW more power than its traditional counterpart. Moreover, the dehumidifier controls the humidity in the linear generator which would increase its lifespan.

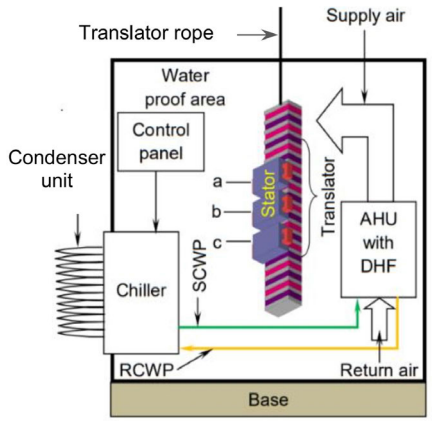

FIGURE 13. Water cooling system for linear generator [31].

Other than these permanent magnets, the compound $Fe_{16}N_2$ known as iron nitride is applied in [32] which exhibits the best performance among all conventional rare earth free permanent magnets. Table 2 presents outcomes of the LG for application of various high graded permanent magnets along with conventional one.

In some cases, the permanent magnet is used in the stator or translator as mentioned in the parenthesis (in Table 2). A comparison is also presented for the electrical parameters considering the existing rare earth free permanent magnet with the highest magnetic energy product and the proposed one.

It can be summarized from this section that, the research in developing permanent magnets results tremendous improvement in designing LGs. For viable operation at higher temperature, traditional permanent magnets are replaced with high graded ones. Moreover, reduction of detent force is obtained with the use of Halbach array. Demagnetization of permanent magnets due to higher temperature is mitigated with the help of water-cooling system. It can further be reduced by using superconductors.

TABLE 2. Outcome of the LG for using high graded permanent magnets.

Permanent magnet	Type of generator	Outcome
Conventional NdFeB N30, N35	PMLG (stator or translator)	➢ Low remanence magnetism ➢ Low coercive force ➢ Low magnetic energy product
N48H (NdFeB)	PMLG (stator)	➢ Output power increased ➢ Costly [26]
N28EH	PMLG (stator)	➢ Increased output power than N35M [27]
Quasi-Halbach array	External tubular PMLG (stator)	➢ Reduced detent force ➢ High efficiency ➢ Appreciably high output power [29]
N52	PMLG (translator)	➢ Remarkably high remanence magnetism ➢ Low coercive force ➢ High energy product [33]

VII. MAGNETIC CORES IN LINEAR GENERATOR

Copper losses and core losses are dissipated as thermal energy which eventually diminishes the remanence magnetism within the permanent magnets. Traditionally, iron cores are used in the permanent magnet linear generator which are often detrimental for high amount of core losses during extraction of wave energy. Moreover, these cores tend to saturate at lower B resulting in low output power. Thus, there is great need of materials which are suitable to be used as magnetic core. Numerous analyses are found where the use of graded cores results noticeable reduction in core loss.

A. APPLICATION OF HIGH-GRADE STEEL CORE

High grade steel core can significantly increase the power generating and reduce the core loss. Thus, it can play vital role of reducing temperature rise in the linear generator because of core loss. High graded steel cores are often classified into non grain oriented and grain oriented. Performances of Armco DI-MAX non-oriented electrical steel M-27 and HF-10 based cores are presented in [34]. Fig. 14 shows the core loss profile and magnetization curves of HF-10, HF-10X, usual steel core, and M-27 cores under 50Hz frequency. M-27 provides better saturation than HF-10 as plotted in Fig. 14(b), but its core loss is noticeably higher than HF-10. Performance of DI MAX HF-10X (called HF-10X herein after) based core is compared with the conventional iron core in [35]. HF-10X shows the lowest core loss and better performance among the others.

High graded permanent magnets and magnetic cores are used in PMLG in [33] to generate/harvest more electrical

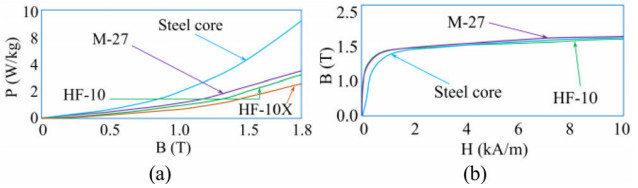

FIGURE 14. Characteristics of HF-10, M-27, and ordinary steel core: (a) core loss and (b) magnetizing curves of different materials.

power/energy from the ocean. Three different core materials are used for the PMLG design: Supermendur core, Vitroperm 500m, and conventional steel. Fig. 15 illustrates the magnetizing curves of three materials. Supermendur core is made of cobalt, vanadium, and iron which demonstrates low coercive force and hysteresis loss. It also exhibits higher permeability and remanence than usual materials. Supermendur is mostly used where the operating temperature is high. On the contrary, Vitroperm 500F is designed to present high magnetic saturation point than conventional iron core.

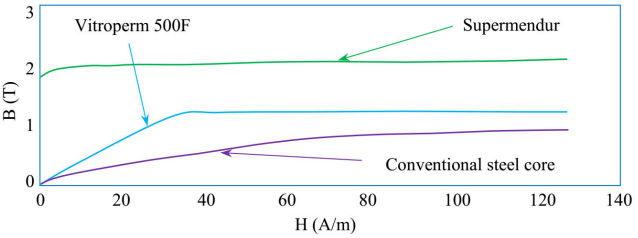

FIGURE 15. Magnetizing curve of conventional steel core, Supermendur, and Vitroperm 500F.

As for the permanent magnet, N38, N52 and traditional NdFeB is used. The current of Vitroperm 500F is much lower than the conventional steel core. On the contrary, the core made of Supermendur performs better than the usual steel core. Moreover, as for terminal voltage, the Supermendur outperforms the other two materials but the terminal voltage of Vitroperm 500F degrades than the usual core. In addition to that, Fig. 16 demonstrates the generated power under same loading conditions. Performance of Vitroperm 500F is the worst among these. On the other hand, performance of Supermendur material surpasses the other two in terms of power generation.

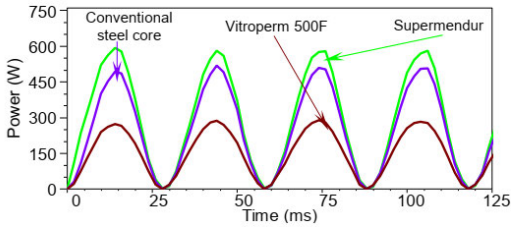

FIGURE 16. Generated electrical power for using different magnetic core.

A high graded magnetic core is demonstrated in [36] which can significantly reduce the core loss of PMLGs. DI MAX HF-12 (called HF-12 herein after), HF-10 and conventional iron as the test material are applied in the PMLG.

Fig. 17 shows magnetizing curves of these materials and the proposed materials have better magnetic saturation property than ordinary iron. Core loss of the generator using HF-12 and the conventional core is illustrated and compared (Fig. 18) where HF-12 exhibits lower core loss. In addition to that, the power generating performance of the PMLG is optimized using human intervened genetic algorithm. Thus, using HF-12, the core loss is decreased by approximately 70.43%. Therefore, HF-12 core based PMLG would produce much more electrical power than traditional iron core type PMLG

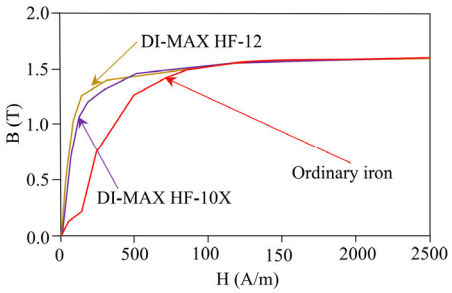

FIGURE 17. Magnetizing characteristics of the conventional, HF-10X, and HF-12 core.

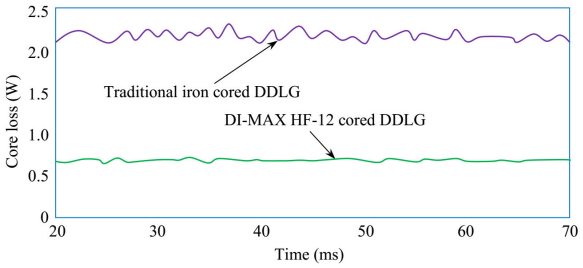

FIGURE 18. Core loss using traditional core and HF-12 core.

Another comparison is presented in [37] where a linear generator with the ordinary steel core, DI-MAX-HF-10, and XFlux material are compared. DI-MAX-HF-10 results much reduction is core loss compared to that of using the ordinary one. Because of using XFlux material, core loss is further minimized by 15.6% again for its good magnetic properties.

B. AIR CORED LINEAR GENERATOR

Air cored LG is often called coreless as there is no iron core in it. Hence, the attraction force caused by the magnetic core and permanent magnet is minimized. A linear double-sided topology for air cored LG is proposed in [38] that can reduce the flux coupling in longitudinal flux LG. By using an air core, attraction forces between mover and stator is eliminated. Moreover, the attraction force that exists within the opposite ends of the translator is reduced which will eventually reduce mass of the LG. Ensuring minimum number of poles and maintaining maximum permissible current density, the optimal dimensions of the LG is determined successfully through exhaustive optimization technique. This structure provides minimum copper and magnet mass. Furthermore, a 1kW

rated protype for validation is developed. The experimental results reveal that around 95% efficiency with approximately unity power factor can be achieved using the proposed structure.

An air-cored tube structured permanent magnet linear generator is proposed in [39] in which cogging force, ratio of radial Lorentz force, and axial Lorentz force are reduced. Furthermore, the proposed generator can deliver higher power than the conventional one. Additionally, a pair of anti-parallel thyristors are used to bypass the inactive coils. Moreover, seven times reduction in thermal loss is achieved unlike any conventional bypass scheme. Also, the thermal loss in the proposed model is not contingent on number of coils.

Another air core LG is presented in [40] where a prototype is built and tested in two different cases. Each section of the stator consists of three windings placed side by side. Total 38 sections are connected in series and are placed in an aluminum ring. Furthermore, two cases are considered for testing purpose. In the first case, there is no overlap between stator and the translator at the stroke end. For the second case, full overlap occurs between the stator and the translator. Two cases are implemented with the help of a crank shaft and a drive motor. The drive motor is used to simulate oceanic waves. Three phase ac supply is initially rectified and further converted to ac waveform to control the frequency. As the frequency varies, the motor speed also changes accordingly. Since, direct connection of a single LG to the grid is not feasible, output of the LG is feed to a dc bus where the dc voltage is regulated. Lastly, it is demonstrated that the zero overlapping case results 46% increase of power to weight ratio.

An approach is adopted in [41] that makes an air cored electric machine retain a concentric arrangement of solenoid-shaped coils, stator, and rotor. This would support manufacture and maintenance. 3D finite element analysis is performed to examine the performance of the machine. Relation between the airgap length and pole numbers through geometrical analysis are determined. The most optimum number of poles for the proposed design is 32. Magnetic and geometric properties are studied using magnetic circuit analysis. Considering thermal environment, the number of turns per phase and rated parameters are examined using electrical circuit analysis. Finally, the machine demonstrates at least 90% efficiency at different operational environment. The proposed machine offers simplicity in terms of construction. The main demerit of this generator is that its power density is much lower than other iron cored conventional machines.

At the end of this section it can be concluded that, reducing core loss is the way to increase efficiency. In case of any LG this is achieved by using high graded steel cores. Moreover, air cored LG can almost reduce core loss that demonstrates an advantage over the iron cored LG. But it is at the rudimentary stage and its size is found quite large compared to its generated power.

VIII. PIEZOELECTRIC GENERATOR

Energy converters or harvesters made of prominent polyvinylidene fluoride materials are used to harness substantial amount of electrical power form the ocean. Energy converters can be used to supply electrical power to applications that are operated in ocean such as different electrical sensing elements, floating harbors, robots etc. The efficiency related to energy conversion of wave energy converters (WECs) can be enhanced by integrating various types of piezoelectric materials. Experiments show that using this methodology, 0.2μW electric power with 2.2V can be acquired by stressing the material with a pressure of 1.196kPa at 20Hz frequency. A piezoelectric WEC is designed, semi-submerged in ocean, and anchored in the seabed [42]. The semi-submerged structure of energy harvester produces vibration corresponding to the oceanic wave's dynamic oscillation. The external force caused by oceanic wave can continuously deform the piezoelectric plates because it is placed on the member of the harvester. Depending on the material of piezoelectric transducer, different level of voltages can be generated by transducing the stresses on the device.

A. PIEZOELECTRIC DEVICES

A cost effective piezoelectric WEC is developed in [43] which consists of piezoelectric disks as illustrated in Fig. 19(a). Flexible cords are used to attach the device with seabed. The converter having the piezoelectric disks rotate because of the oscillating motion of oceanic wave. The piezoelectric disk transduces the kinetic energy of the oceanic wave into electrical energy. Inside the device, a pendulum is place so that it can enhance the warp of the piezoelectric strips. Fig. 19(b) shows a WEC, proposed in [44], that integrates a piezoelectric bar comprised of lead zirconate titanate (Pb[Zr(x)Ti(1-x)]O3 where, $0 \leq x \leq 1$).

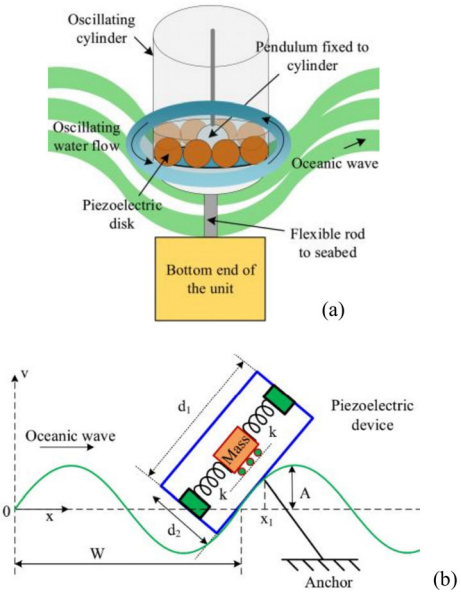

FIGURE 19. Piezoelectric WEC: (a) disk shaped and (b) bar shaped.

The external force caused by oceanic wave is amplified by a vertical lever which is attached to the piezoelectric bar. A mass-spring arrangement is adopted to create vibration from wave oscillations. Two piezoelectric members are connected to the mass by springs. The purpose of using the spring is to avoid direct collision between the mass and the disk. Also, it gradually increases or decreases the stress on the disk.

When the device experiences an oscillating wave, vibration is created due to the movement of the mass inside the device. As a result, the member experiences continuous deformation caused by vibration. Thus, vibration is transduced into electrical power through piezoelectric materials. Piezoelectric materials can generate electrical power if the heave and pitch motion of oceanic waves are utilized. It employs a floating buoy which is tied to the seabed by connecting rope as illustrated in Fig. 20 [45]. The piezoelectric device on the left is mounted to the connecting shaft of the buoy. Therefore, any heaving motion of the buoy creates rolling motion in the device. As it experiences rolling motion, the pendulum tends to deform the piezoelectric disks which results in generation of electrical power. Many small sized devices are connected to the shaft which would appear as a branch of a tree having leaves on it. Therefore, small portion of electrical energy coming from each of the devices accumulates into a large amount of energy. The buoy situated at the right-hand side (Fig. 20) encapsulates the piezoelectric device. If the buoy encounters pitching motion, then the pendulum also moves accordingly and creates stress on the disks. Hence, electrical energy is obtained from both heaving and pitching motion.

Another type of piezoelectric harvester is proposed in [45] using four disks made of lead zirconate titanate along with a balanced type pendulum. These devices are also known as flexible piezoelectric device (FPED). Each of these elements are confined in a carrier box made of brass material. In Fig. 20, the device is located inside the box and labeled as ''Energy harvesting unit''. Water can easily enter the box or can easily go out from the device which disturbs the balanced position of the pendulum.

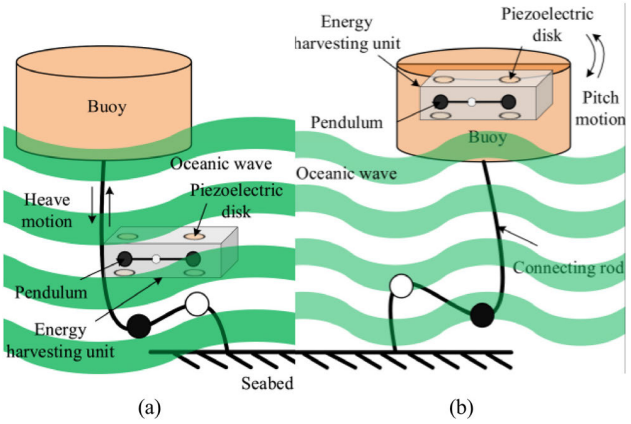

FIGURE 20. WEC using (a) heave and (b) pitch motion of sea waves.

Thus, the pendulum creates stress on FPED and hence it gets deformed with electrical power generation. A piezoelectric material based oceanic energy harvester is designed in [46] which is illustrated in Fig. 21. The harvester is placed just beside a vertical oceanic cliff. It comprises of vertically placed piezoelectric thin plates which get stressed when oceanic waves pass through them. Consequently, wave motion is transduced into electrical energy and passed to external circuitry.

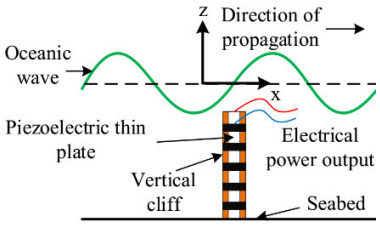

FIGURE 21. (a) Experimental tests of elastic floating unit with hanging structure placed beside a vertical oceanic cliff.

An experimental test on elastic floating unit with hanging structure is conducted in water tanks in [47]. Both floating type and submerged type buoys are used in the test which are depicted in Fig. 22(a). The height and width of the test float is 115mm and 85mm, respectively. An artificial wave is created in a wave tank having an amplitude of 0.077m and 1m wavelength. The FPED is mounted on the top of the float for submerged type devices. In case of floating type device, it is placed at the bottom of the floats. For both submerged and floating type devices, connecting ropes/rods are used to attach the devices with the tank. Since, FPEDs are made of polyvinylidene fluoride material, efficacious electrical performance can be obtained by choosing the length of the polyvinylidene fluoride layer from 0.1mm to 0.5mm, but it is recommended not to exceed 0.5mm.

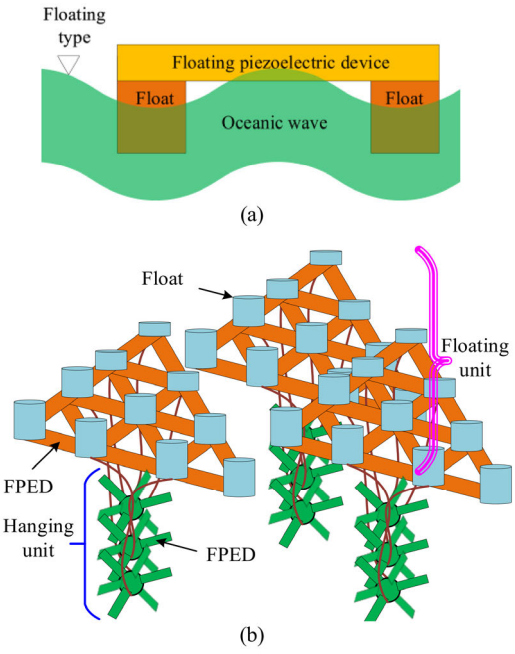

FIGURE 22. Elastic floating unit with hanging structure: (a) single device and (b) aggregated structure.

B. AGGREGATED FORM

A single piezoelectric device produces extremely small amount of power. To increase power, these devices are needed to be accumulated. Thus, an aggregated form of elastic floating unit with hanging structure (EFHAS) is proposed in [47] which can harvest oceanic energy. It consists of a hanging and a floating section as illustrated in Fig. 22(b).

The floating branches are connected to each other by flexible piezoelectric device. There are few vertical and horizontal branches of flexible piezoelectric device in the hanging section that can generate electrical power from the heaving motion of oceanic wave. This device can generate power even from weak oceanic waves which is highly beneficial. Wind ocean farm can be established where a series of EFHAS surrounds the offshore wind turbines. Therefore, wind turbines extract wind energy and the EFHASs harness oceanic wave energy from the ocean. This combination is advantageous since the EFHAS can absorb the vigorous power of oceanic waves thus protecting the wind turbines.

Piezoelectric devices are effective to harvest wave energy. To get proper deformation from oceanic waves, various shapes of piezoelectric devices are formed. Disk and bar shapes are remarkable of them. These devices successfully harvest energy from heaving and pitching motion of the oceanic waves. Moreover, the vertical cliffs can also be used for power generation. Since the power output of a single device is in μW range, these devices are combined to create a large structure that is capable of generating high amount of power.

C. MATHEMATICAL MODELS OF PIEZOELECTRIC AND TRIBOELECTRIC NANOGENERATOR

The mathematical models of two generators namely piezoelectric and triboelectric nanogenerator are tabulated in Table 3. The model describes the parameters of output voltage, current transport, and displacement current.

TABLE 3. Mathematical model of Piezoelectric and triboelectric nanogenerator.

Parameters	Piezoelectric	Triboelectric
Output voltage	$V_{OC} = z\sigma_p(z)/\varepsilon$	$V = \sigma_1(z,t)\left[\frac{d_1}{\varepsilon_1} + \frac{d_2}{\varepsilon_2}\right] + z\left[\sigma_1(z,t) - \sigma_{C]}\right]/\varepsilon_0$
Current transport equation	$RA\frac{d\sigma}{dt} = z\left[\sigma_p(z) - \sigma(z)\right]/\varepsilon$	$RA = \frac{z\sigma_c}{\varepsilon_0} - \sigma_1(z,t)\left[\frac{d_1}{\varepsilon_1} + \frac{d_2}{\varepsilon_2} + z/\varepsilon_0\right]$
Displacement current (J)	$J_{Dz} = \frac{\partial\sigma_p(z)}{\partial t}$	$J_D = \frac{\partial\sigma_1(z,t)}{\partial t}$

In table 3, z denotes displacement along z-axis, σ_p denotes polarization charge sensitivity, ε indicates the permittivity of the dielectric whereas ε_0 signifies the permittivity of vacuum. Also, R denotes the load resistance, A is the cross-sectional area of the electrode, displacement current is J_D, d_1 and d_2 are the thickness of two different dielectric materials of TENG whereas ε_1 andε_2 are permittivity of the corresponding materials. Also, σ_C denotes surface charge sensitivity and σ_1 signifies charge accumulation in the two electrodes, V_{oc} denotes output open circuit voltage.

IX. TRIBOELECTRIC GENERATOR

A single unit of triboelectric nanogenerator (TENG) can produce small amount of power. It has first been developed in 2006 and after various improvements such as electrostatic induction and coupling of triboelectrification, it emerged as a compelling transducer in 2012 [48]. TENG generates current with the help of changing polarization field. The field is induced by surface polarization charges which is an underlying principle of Maxwell's displacement current. TENG outperforms electromagnetic generators (EMG) in terms of light weight, reduced fabrication cost, higher efficiency, and increased power density [49]. Moreover, a single TENG could provide a power density of around 500Wm^{-2} with an efficiency of 70% which is sufficient to operate small electronic device [50]. Due to its high-level of power density, it has become a prominent technology with high potential for harvesting OWE.

A. ROLLING BALL BASED TENG

Since, oceanic waves have low frequency (<2Hz) and intermittent nature [51], the electromagnetic generators prove to become ineffective. This is because of its high mass density and its propeller-based technology. In contrast, TENG has low mass density and incorporates electrostatic induction technology. Moreover, TENG can generate more power in lower frequencies as compared to EMG. However, EMGs power generating capability is higher than TENG at higher frequencies. The working principle is shown in Fig. 23 where a nylon ball having positive charge is enclosed by a Kapton film which separates the ball from two outer electrodes. Behind the Kapton film, there are two arc shaped stationary electrodes which get energized when the ball rolls forward or backward in the shell. When the ball is at rest, there is no charge imbalance hence no current is flown. However, if the ball starts to roll forward, then it repels positive charges from the electrode (right hand) and negative charges will flow from electrode (left hand) towards the other electrode through the load. In [52], both experimental and simulated

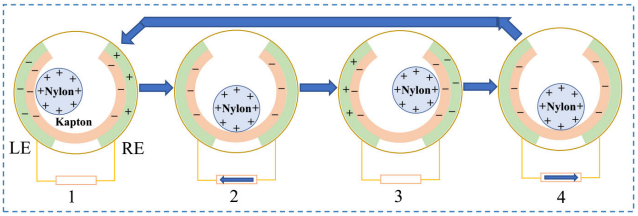

FIGURE 23. Working principle of rolling ball based TENG.

approaches are described in order to find the optimized size for the nylon ball. The results show that the optimized size of the nylon ball is 4cm and the device can operate around 70 LEDs using wave energy. Moreover, significant amount of power can be generated if the frequency of the wave is within 1.23Hz to 1.55Hz.

Again, if the ball starts to roll backwards then the opposite events occurs. Thus, movement of the ball is converted into electrical energy. Hence, if there are random external vibrations, TENGs are suitable to convert the motion into electrical energy. It can be encapsulated into a sealed structure where no water from the ocean can come in contact. As these devices generate extremely low amount of power, therefore, numerous TENGs are connected with each other to generate significant amount of power from the ocean. Furthermore, due to its light weight, TENGs can easily float and absorb the oceanic wave motion. Voltage, current, and power of an EMG highly depend on frequency of the mover whereas the voltage of TENG depends on system capacitance and electrostatic charge buildup. A threshold frequency is introduced in [12] which is approximately 5Hz. If an EMG and a TENG of equivalent size is operated, then TENG generates more power than EMG provided that the frequency is less than the threshold value. However, EMG performs better beyond the threshold frequency. On the contrary, another minimum frequency is required to maintain below which an EMG struggles to produce any sort of power. This is due to diode rectifier, as diodes create a voltage drop of around 0.5V. However, TENGs could generate around 20–50V which is enough to produce power even after the diode voltage drop.

B. FOUR DIFFERENT MODES OF TENG

Four different modes of TENG are described in [12] and is shown in Fig. 24. First mode is freestanding triboelectric layer in which two electrodes are symmetrically placed either vertically or horizontally as in Fig. 24(a), where two horizontally placed electrodes exist.

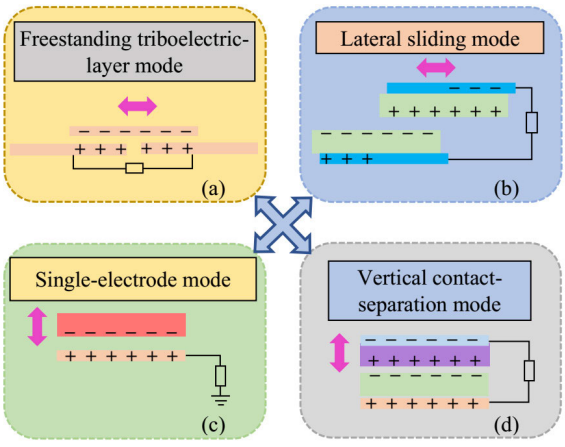

FIGURE 24. Four different modes of bar shaped TENG.

A triboelectric plate is present which can slide horizontally with external force and is able to create charge imbalance between two stationary electrodes. On the contrary, if the electrodes are placed vertically while facing each other, then the triboelectric plate must move vertically between the gap. The output of this mode is ac whether the electrodes are placed vertically or horizontally.

The second mode of TENG is lateral sliding mode. This mode is similar to vertical contact-separation mode in terms of construction. Here, one of the plates slides along the horizontal direction because of external force as depicted in 24(b). The triboelectric charge on the electrodes create a potential difference which drives the load current. If back and forth sliding takes place, an ac output can be obtained from it.

A single electrode mode is demonstrated in Fig. 24(c) which can move with respect to applied external force. On the other end, an electrode is placed which is connected to a load. If the moving plate gets closer, then there would be an imbalance in electric field distribution of the electrodes which would result in charge exchange. Although this mode can operate from any sort of movement of the plate, the resulting current is quite small which makes it very ineffective. However, this mode can be used in some miniaturized active sensors which can sense the presence of any charged object.

Fourth is vertical contact-separation mode as depicted in Fig. 24(d) in which two plates of distinct materials having different triboelectric polarities are placed in opposite to each other. One of the two plates must be made of dielectric material which is connected to an electrode. The other plate is conductive and therefore it can act as an electrode by itself. When an external force is applied to either of the plates, then the gap between them diminishes. Consecutively, both the plates contain opposite charges on their surfaces. When the force is released, the gap between the plates increases and voltage drop occurs which is applied to the external load. If the gap is closed again, the voltage difference created by triboelectric charges disappears. Therefore, to acquire charge equilibrium, the electrons flow in the opposite direction. Due to its increased power density and simple construction, this mode of TENG is suitable for periodic motions and vibrations.

C. WAVY SHAPED TENG

Since the TENGs are susceptible to corrosion, the idea of fully enclosed TENGs have emerged. Different types of fully enclosed TENGs are introduced in [12]. The first of them is wavy electrode TENG which has wavy shaped Kapton sandwiched between wavy shaped copper layers. The wavy shape is placed between two nanostructured polytetrafluoroethylenes as shown in Fig. 25(a). Since the wavy shape is flexible, any vertical force can easily be converted into lateral displacement. As a result, sliding between nanostructure and wavy structure create potential difference between the electrodes as presented in Fig. 25(b). When force is removed and the wavy shape returns to its original shape, sliding between two structures occurs again, but in reverse direction. Compression and expansion of the wavy structure creates ac current. Thus, this device can convert the water impact energy of oceanic wave into electrical energy. Experiments show

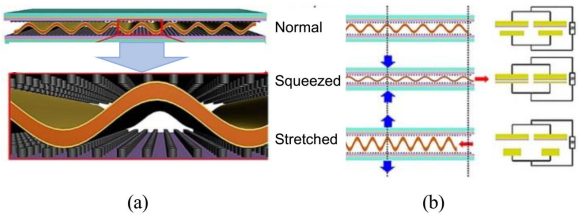

FIGURE 25. Wavy shape TENG: (a) placed between two polytetrafluoroethylene and (b) its illustration [12].

that a wave of 0.2m amplitude having a speed of 1.2m/s can provide 30V and 6μA using wavy TENG. Hence, this is a promising device for oceanic wave energy conversion.

D. DUCK SHAPED TENG

Duck shaped TENG and its multilayer form are illustrated in [53] where nylon balls are placed on Kapton films and electrodes are placed beneath the films. The structure of the TENG mimics the salter's duck which can convert wave energy into electrical energy. From Fig. 26, positively charged nylon balls roll back and forth and ac current passes through the electrodes accordingly. The sequence of operation is clockwise.

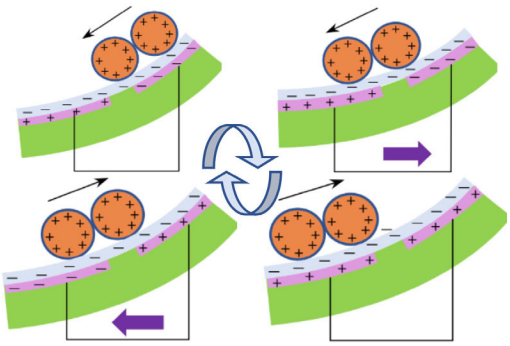

FIGURE 26. Working principle of duck shaped TENG.

The triboelectric nanogenerators which are discussed can generate very low amount of power for a single unit. However, if numerous TENGs are integrated to create a network, then its network can generate substantial amount of power. Moreover, network of TENGs can be used to harvest oceanic wave energy from undercurrents as well as surface waves unlike its EMG counterpart. Furthermore, most of the oceanic waves are multidirectional which makes network of TENGs suitable for harvesting OWE. Network of TENGs can easily be arranged in both epicontinental sea and in offshore locations. A hybrid TENG is developed in [54] which is a combination of rotational disk based TENG and a liquid solid contact TENG.

The disk based TENG shown in Fig. 27 can utilize the irregular rotational motion and its power density is approximately 42.6Wm^{-2} at 1000rpm speed. The liquid solid contact TENG operates using the vertical contact separation mode. Water and polydimethylsiloxane create potential difference between the copper electrodes because of continuous contact

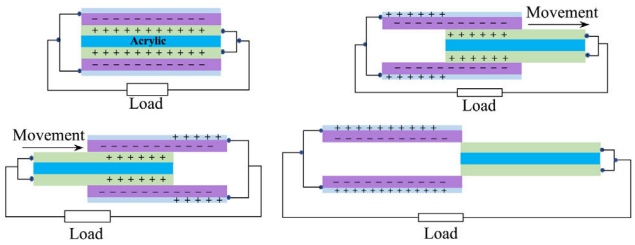

FIGURE 27. Operation of the disk based TENG.

and separation. Its power density is 50mWm^{-2} at 5Hz. The hybrid TENGs are expected to be able to extract current motion from the ocean.

A swing structured TENG is simulated and tested in [55] for wave energy extraction. The device exhibited 0.48mW of average power. Using wave energy, the device successfully powered transportable electronic devices through which temperature and other environmental assessments are carried out. A spherical ball based multilayer TENG in [56] is used to extract energy from multidirectional water wave. Assisted structure with six springs along with power management module enables it to demonstrate maximum output of 8.5mW with 250V, and 80μA. Another spherical ball based TENG network shown in Fig. 28(a) is proposed in [57] where millions of spherical TENGs are integrated to form a structure which looks like fishing net. Coupling the TENGs can enhance the charge output by 10 times as demonstrated in [58]. Also, different types of mechanical connections between the TENGs such as rigid, string, and elastic coupling are used and analyzed. Among these connections, elastic type connection has outperformed the other two. To boost the output current of the network, the electrical connection among two adjacent TENGs are in parallel which forms a string of TENGs. Moreover, to enhance the output voltage of the network, each string is connected in parallel with other strings which eventually create an array of TENGs. If 1km^2 off area is covered by this network, then approximately 1.15MW of power can be generated.

FIGURE 28. Aggregated form of TENG: (a) a spherical ball based TENG network. (b) combined arrangement with other RESs [57], [59].

When wave energy converter technology will improve in the future, then the sea area can be utilized to extract energy from wave, wind, and solar as shown in Fig. 28(b) [59]. Thus, two third of the world's area which is covered by ocean can be utilized properly to harvest blue energy. A single TENG is unable to produce high amount of power. Usually it can generate a power of few nanowatts. This generator also

produces extremely low amount of current while producing a lot of harmonics.

From the discussion on TENG, it is understood that these small sized devices can easily harness energy from the random motion of the ocean. The output of these individual devices is infinitesimal as compared to electromagnetic generators. Hence, interconnecting these devices must be accomplished to obtain significant amount of power.

X. GRID INTEGRATION

Since the oceanic wave varies in nature, the output voltage and frequency are also change. Hence, the output of the linear generator cannot be connected to load or grid directly. Thus, an intermediate converter stage is required which rectifies the output of the linear generator and also uses an inverter by which the voltage and frequency can correspond with the load or grid. Fig. 29 shows a general block diagram of power flow in wave energy conversion system.

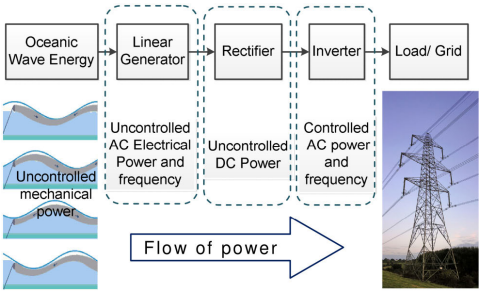

FIGURE 29. Block diagram of power flow [23].

Fuzzy logic controller is used in [60] to control the output voltage of a linear generator. An inverter is integrated which controls the modulation index of its pulse width modulation. The whole system is simulated in MATLAB/Simulink where the voltage, current, and power waveforms are demonstrated. At the topmost and bottom-most position of the translator, there is no relative velocity which results in zero output voltage. The control of modulation index of the inverter is shown in Fig. 30(a). The value of modulation index remains between 0–1. Output voltage across the load with and without fuzzy logic controller is plotted in Fig. 30(b). The load voltage remains consistent when the controller is applied. It is mentioned that the proposed controller can also be used in other rotating generators for wave energy converter. Even though ripples are seen in the voltage waveform caused by discrete solver, a continuous solver can effectively solve this problem.

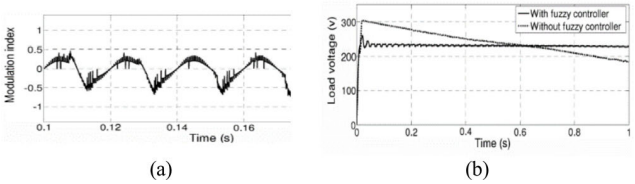

FIGURE 30. Control: (a) Modulation index control and (b) waveforms.

An advanced controller is proposed in [61] which reduces most higher and lower order of harmonics thus safeguarding the quality of electrical power. One key advantage of this controller is that, it integrates line filter of very small size. The total harmonic distortion and the fast Fourier transform of the output voltage are measured and compared with a preset tolerance. Moreover, instead of using a feedback control, a feed forward control is utilized which results in faster response. From Fig. 31(a) it is observed that for the carrier frequency of 3kHz, there is ripple of the output voltage which is pointed out by circles. Fig. 31(b) shows the output voltage waveforms of both the proposed and conventional converters for almost the same carrier frequency.

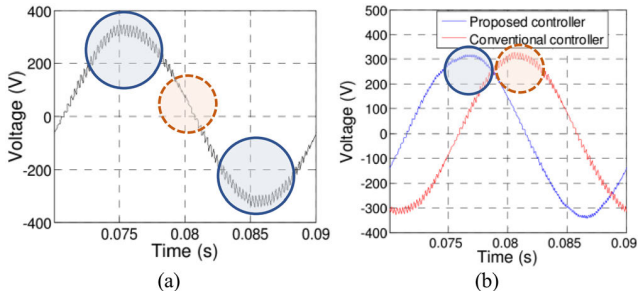

FIGURE 31. Voltage waveforms: (a) conventional (3kHz) and (b) proposed controller.

The waveform for the proposed controller contains significantly less ripples than that of the conventional space vector modulation. MATLAB/Simulink is used to simulate the results. Furthermore, the proposed modulation is compared with advanced pulse width modulation and space vector modulation. The magnitude of voltage harmonics for the conventional controller is illustrated in Fig. 32(a) and the same for the proposed controller is shown in Fig. 32(b).

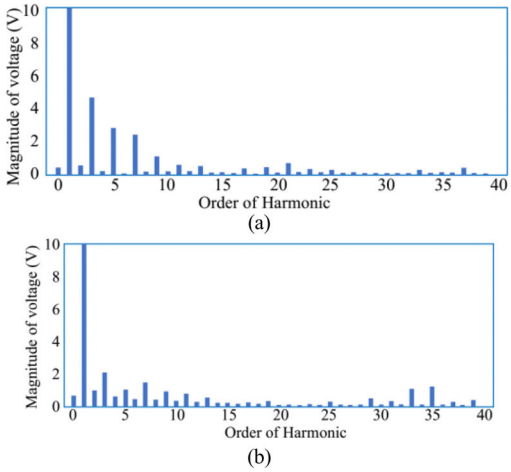

FIGURE 32. Voltage harmonics for (a) the conventional and (b) the proposed controller.

The proposed fuzzy logic controller outperforms the conventional one. The proposed scheme effectively eliminates

the harmonic distortion. To represent the performance of the proposed converter, the conventional converter requires carrier frequency with approximately double frequency. Since the proposed converter requires less carrier frequency, the switch loss is reduced significantly.

Integrating the generated power into electrical grid is as significant as generating the power. The volatile output from wave energy converters need to be regulated through some effective controllers. Furthermore, to eliminate the harmonics and maintain the frequency, power electronic devices such as rectifier and inverters are essential.

XI. DISCUSSION

The outcomes of using advanced magnetic cores over the conventional one in various LGs (which is basically an EMG) are summarized in Table 4.

TABLE 4. Outcome of the LG for using high graded magnetic cores.

Magnetic core	Type of Generator	Outcome/Feature/Properties
Traditional	PMLG (stator and translator)	➢ High magnetic saturation point ➢ High core loss
Armco DI-Max M-27	PMLG (stator and translator)	➢ Core loss lower than conventional core [34] ➢ Saturation characteristics is better than HF-10 ➢ Core loss higher than HF-10 [24]
Armco DI-Max HF-10	PMLG (stator and translator)	➢ Core loss lower than M27 [34] ➢ Higher mechanical strength [24] ➢ Better magnetic saturation property than conventional core [36]
Armco DI-Max HF-10X	PMLG (stator and translator)	➢ core loss is reduced to 33.2% ➢ Stronger and more efficient [35]
Armco DI-Max HF-12	PMLG (stator and translator)	➢ Better magnetic saturation property than HF-10 ➢ Lower core loss (reduced to 29.57% after optimization) [36]
Supermendur	PMLG (stator and translator)	➢ Low coercive force and hysteresis loss ➢ Higher permeability and remanence ➢ Higher terminal voltage [33]
Vitroperm 500m	PMLG (stator and translator)	➢ High magnetic saturation point than traditional core ➢ Lower current and terminal voltage than traditional core [33]
Air core	Tubular PMLG (stator)	➢ Cogging force and attraction force are reduced ➢ Ratio of radial Lorentz force and axial Lorentz force is decreased ➢ Higher output power ➢ Thermal loss reduced by seven times [39]
Air core	Longitudinal flux LG (stator)	➢ Attraction forces reduced ➢ Efficiency is remarkably high with 5% of power loss [38]
Air core	PMLG (stator)	➢ Zero overlapping region increases power to weight ratio by 46% [40] ➢ Highly effective with around 10% power loss [41]

The other two types of generators can produce low amount of electrical power which is not even comparable to the LG. Therefore, most of the research is conducted regarding improvement of the LG in different way, on their structure, material, way of implementation, etc. Application of high graded magnetic material significantly enhance the performance in two ways. One is generating high power, the other is minimizing core loss.

Electrical power from the electromagnetic, piezoelectric, and electrostatic generators depend on wave frequency. As the wave frequency gets increased, the output of generators also increases. In case of TENG, this increase is linear, but the output of EMG increases exponentially. For this reason, at higher frequency, EMG generates enormous amount of power.

A comparison of each type of generator with the properties are summarized in Table 5.

TABLE 5. Comparison among different types of electrical generators.

Properties	EMG	Piezoelectric Generator	TENG
Durability	High	Low	Low
Physical strength	Strong	Weak	Weak
Weight (single unit)	Heavy weight, in order of several kilograms	Light weight, in order of grams	Light weight, in order of grams
Shape	Cylindrical, or rectangular solid	Cylindrical, flat, or rectangular solid	Spherical, or rectangular solid
Geometry (single unit)	Large, mostly in order of m	Very small, mostly in order of mm	Small, in order of cm
Sustainable position	Mostly submerged	Floating and submerged	Floating and submerged
Installation	Difficult	Easy	Easy
Output voltage (single unit)	High, example: (660V) [62]	Low, example: (3.3V) [45]	Low, example: (30V) [12]
Internal resistance	Low, few ohm (Ω)	High	High
Output current	High, example: (875A) [62]	Low	Low (around 6μA) [12]
Filter requirement	Low	High	High
Scale of power production	kW to MW range, example: (1MW) [62]	μW to mW	μW to mW
Power-frequency characteristics	Exponential	Linear	Linear
Power density	83.33kWm^{-3} [62]	2–6mWm^{-2} [63] 0.5Wm^{-3} [44]	500Wm^{-2} [50] 4.81Wm^{-3} [56]
Cascading	Optional	Essential	Essential
Approaches	Shape and design optimization, use of superconductor in coil, use of graded PM and core material, using cooling system	Element optimization [11], vertical cliff utilization [46], disk shape, bar shape, used as protective means	Ball shape, duck shape, wavy shape, bar shape, disk shape, four different modes

From the study it is found that, there are total three fundamental principles of electrical power generation from the oceanic wave. They are electromagnetic induction, piezoelectric, and triboelectric which are discussed elaborately in this

review. In fact, LG is mostly utilized to harvest oceanic wave in several projects where permanent magnet LG is widely used. A single unit of this type of generator has the ability to produce up to megawatt scale of electrical power. This type of generator operates on the principle of electromagnetic induction where resistive free electron conduction is driven by Lorentz force.

From the comparative structure as depicted in Table 5, it can be concluded that the fishnet structure is suitable for lightweight and small structure such as TENG. On the other hand, because of having large and heavyweight structure, electromagnetic generators require separate buoy or floating structure. Piezoelectric generators require different type of supporting structure so that it make significant deformation to produce electricity.

Dielectric elastomer, a group of electroactive polymers, is investigated in the late 1990s. It is elastic, lightweight, and can convert electric energy into mechanical energy. This device can also be used for generating electrical power from the oceanic wave although this type of WEC is still not found so far.

XII. CONCLUSION

Although electrical power can be generated from the oceanic wave by various types of generators, careful analysis is required for proper selection. Each type of generator has side by side pros and cons. EMG exhibits excessive current due to its lower internal resistance which would result in overheating the device. Moreover, its large structure and high mass density makes it quite heavy.

Piezoelectric generator produces μW to mW power with a single unit or device compared to traditional electrical generator. It utilizes the rolling and heaving motion of the waves. Polarization charges are created with the help of vertical mechanical deformation. With inadequate efficiency, the piezoelectric generators provide low leveled pulsating output. Its structure is small and fragile. To attach the device with the seabed, piezoelectric devices occasionally use ropes which may get frayed whereas LGs use anchors that retains high strength. Filters are required since the output will have many harmonics. Furthermore, the durability of this generator is inadequate.

TENG works on the principle of electrostatic induction with contact electrification. The slight motion of electrostatic charges and time dependent electrostatic induction produces capacitive displacement current. It can harvest energy from low frequency waves. Additionally, the random movements caused by oceanic waves can also be converted into electrical energy. Unlike LG, TENGs are easier to manufacture and install. It demonstrates higher efficiency at low frequencies. Moreover, various materials can be incorporated with different working modes. The fishnet like structure of TENG network requires a lot of space. Large vessels are required to go around these which creates difficulties. Many marine creatures may get tangled into this structure. Additionally, identifying a faulty TENG in the network is quite difficult. To eliminate the harmonics generated at the output, high quality filters are needed. Oceanic wave with high frequency degrades its performance. It can widely be used as sensors.

Piezoelectric generator which is widely used as sensor is suitable for floating and submerged type devices. It can act as a barrier to prevent damage to various devices caused by waves of severe magnitude. TENG is relatively a novice technology which requires more research to flourish. Finally, it can be concluded that, EMG specially LGs are dominating WEC considering the amount of electrical power generation.

REFERENCES

[1] H. Shakouri G., "The share of cooling electricity in global warming: Estimation of the loop gain for the positive feedback," *Energy*, vol. 179, pp. 747–761, Jul. 2019.

[2] O. Farrok, K. Ahmed, A. D. Tahlil, M. M. Farah, M. R. Kiran, and M. R. Islam, "Electrical power generation from the oceanic wave for sustainable advancement in renewable energy technologies," *Sustainability*, vol. 12, no. 6, p. 2178, Mar. 2020.

[3] M. M. Farah, O. Farrok, and K. Ahmed, "Kool Mμ powder core used in a flux switching linear electrical machine for electricity generation from the oceanic wave," in *Proc. IEEE Int. Conf. Power, Elect., Electron. Ind. Appl. (PEEIACON)*, Dhaka, Bangladesh, Nov./Dec. 2019, pp. 127–130.

[4] A. Clément, P. McCullen, A. Falcão, A. Fiorentino, F. Gardner, K. Hammarlund, G. Lemonis, T. Lewis, K. Nielsen, S. Petroncini, M.-T. Pontes, P. Schild, B.-O. Sjöström, H. C. Sørensen, and T. Thorpe, "Wave energy in Europe: Current status and perspectives," *Renew. Sustain. Energy Rev.*, vol. 6, no. 5, pp. 405–431, Oct. 2002.

[5] A. Muetze and J. G. Vining, "Ocean wave energy Conversion–A survey," in *Proc. Conf. Rec. IEEE Ind. Appl. Conf. 41st IAS Annu. Meeting*, Tampa, FL, USA, Oct. 2006, pp. 1410–1417.

[6] *U.S. Marine and Hydrokinetic Renewable Energy Roadmap*, New York, NY, USA, Ocean Renewable Energy Coalition, 2011.

[7] *Mapping and Assessment of the United States Ocean Wave Energy Resource*, Electric Power Research Institute (EPRI), Palo Alto, CA, USA, 2011.

[8] D. Zhang, W. Li, and Y. Lin, "Wave energy in China: Current status and perspectives," *Renew. Energy*, vol. 34, no. 10, pp. 2089–2092, Oct. 2009.

[9] L. Ran, M. Mueller, C. Ng, P. Tavner, H. Zhao, N. Baker, S. McDonald, and P. McKeever, "Power conversion and control for a linear direct drive permanent magnet generator for wave energy," *IET Renew. Power Gener.*, vol. 5, no. 1, pp. 1–9, Jan. 2011.

[10] Y. Li and Y.-H. Yu, "A synthesis of numerical methods for modeling wave energy converter-point absorbers," *Renew. Sustain. Energy Rev.*, vol. 16, no. 6, pp. 4352–4364, Aug. 2012.

[11] H. Li, C. Tian, and Z. D. Deng, "Energy harvesting from low frequency applications using piezoelectric materials," *Appl. Phys. Rev.*, vol. 1, no. 4, Dec. 2014, Art. no. 041301.

[12] R. Li, Y. Li, Y. Zhao, Y. Li, and Y. Li, "Harvest of ocean energy by triboelectric generator technology," *Appl. Phys. Rev.*, vol. 5, no. 3, Sep. 2018, Art. no. 031303.

[13] L. Huang, H. Yu, M. Hu, C. Liu, and B. Yuan, "Research on a tubular primary permanent-magnet linear generator for wave energy conversions," *IEEE Trans. Magn.*, vol. 49, no. 5, pp. 1917–1920, May 2013.

[14] I. A. Ivanova, O. Agren, H. Bernhoff, and M. Leijon, "Simulation of wave-energy converter with octagonal linear generator," *IEEE J. Ocean. Eng.*, vol. 30, no. 3, pp. 619–629, Jul. 2005.

[15] J. F. Pan, Y. Zou, N. Cheung, and G.-Z. Cao, "On the voltage ripple reduction control of the linear switched reluctance generator for wave energy utilization," *IEEE Trans. Power Electron.*, vol. 29, no. 10, pp. 5298–5307, Oct. 2014.

[16] J. Engström, V. Kurupath, J. Isberg, and M. Leijon, "A resonant two body system for a point absorbing wave energy converter with direct-driven linear generator," *J. Appl. Phys.*, vol. 110, no. 12, Dec. 2011, Art. no. 124904.

[17] O. Farrok and M. M. Ali, "A new technique to improve the linear generator designed for oceanic wave energy conversion," in *Proc. 8th Int. Conf. Electr. Comput. Eng.*, Dec. 2014, pp. 714–717.

[18] O. Farrok, M. R. Islam, K. M. Muttaqi, D. Sutanto, and J. Zhu, "Design and optimization of a novel dual-port linear generator for oceanic wave energy conversion," *IEEE Trans. Ind. Electron.*, vol. 67, no. 5, pp. 3409–3418, May 2020.
[19] O. Farrok, M. R. Islam, M. R. I. Sheikh, Y. Guo, and J. G. Zhu, "A split translator secondary stator permanent magnet linear generator for oceanic wave energy conversion," *IEEE Trans. Ind. Electron.*, vol. 65, no. 9, pp. 7600–7608, Sep. 2018.
[20] O. Farrok, M. R. Islam, M. R. I. Sheikh, Y. G. Guo, and J. G. Zhu, "Design and analysis of a novel lightweight translator permanent magnet linear generator for oceanic wave energy conversion," *IEEE Trans. Magn.*, vol. 53, no. 11, pp. 1–4, Nov. 2017.
[21] O. Farrok, M. R. Islam, Y. Guo, J. Zhu, and W. Xu, "A novel design procedure for designing linear generators," *IEEE Trans. Ind. Electron.*, vol. 65, no. 2, pp. 1846–1854, Feb. 2018.
[22] Z. H. Wu and J. X. Jin, "Characteristic analysis of HTS linear synchronous generators designed with HTS bulks and tapes," *IEEE Trans. Appl. Supercond.*, vol. 24, no. 5, pp. 1–5, Oct. 2014.
[23] O. Farrok, M. R. Islam, M. R. Islam Sheikh, Y. Guo, J. Zhu, and W. Xu, "A novel superconducting magnet excited linear generator for wave energy conversion system," *IEEE Trans. Appl. Supercond.*, vol. 26, no. 7, pp. 1–5, Oct. 2016.
[24] S. Molla, O. Farrok, M. R. Islam, and K. M. Muttaqi, "Analysis and design of a high performance linear generator with high grade magnetic cores and high temperature superconducting coils for oceanic wave energy conversion," *IEEE Trans. Appl. Supercond.*, vol. 29, no. 2, pp. 1–5, Mar. 2019.
[25] M. S. Bashir and O. Farrok, "Yttrium barium copper oxide superconductor used in a linear generator for high power generation from the oceanic wave," in *Proc. Int. Conf. Electr., Comput. Commun. Eng. (ECCE)*, Feb. 2019, pp. 1–5.
[26] M. S. Bashir and O. Farrok, "Generation of electrical power by using high graded permanent magnet linear generator in wave energy conversion," in *Proc. 1st Int. Conf. Adv. Sci., Eng. Robot. Technol. (ICASERT)*, Dhaka, Bangladesh, May 2019, pp. 1–5.
[27] M. S. Bashir and O. Farrok, "Harvesting oceanic wave energy by a linear generator using high graded N28EH permanent magnets," in *Proc. 4th Int. Conf. Electr. Eng. Inf. Commun. Technol. (iCEEiCT)*, Dhaka, Bangladesh, Sep. 2018, pp. 514–518.
[28] C. Liu, H. Yu, M. Hu, Q. Liu, and S. Zhou, "Detent force reduction in permanent magnet tubular linear generator for direct-driver wave energy conversion," *IEEE Trans. Magn.*, vol. 49, no. 5, pp. 1913–1916, May 2013.
[29] C. Liu, L. Huang, S. Zhou, Q. Liu, M. Hu, and H. Yu, "Research on a permanent magnet tubular linear generator for direct drive wave energy conversion," *IET Renew. Power Gener.*, vol. 8, no. 3, pp. 281–288, Apr. 2014.
[30] O. Farrok, M. R. Islam, M. R. I. Sheikh, Y. G. Guo, J. G. Zhu, and W. Xu, "Analysis and design of a novel linear generator for harvesting oceanic wave energy," in *Proc. IEEE Int. Conf. Appl. Supercond. Electromagn. Devices (ASEMD)*, Shanghai, China, Nov. 2015, pp. 272–273.
[31] S. Molla and O. Farrok, "Water cooled chiller based HVAC system used in a linear generator for oceanic wave energy conversion," in *Proc. 1st Int. Conf. Adv. Sci., Eng. Robot. Technol. (ICASERT)*, Dhaka, Bangladesh, May 2019, pp. 1–6.
[32] S. Molla, O. Farrok, M. R. Islam, and K. M. Muttaqi, "Application of iron nitride compound as alternative permanent magnet for designing linear generators to harvest oceanic wave energy," *IET Electr. Power Appl.*, vol. 14, no. 5, pp. 762–770, May 2020.
[33] S. Molla and O. Farrok, "Vitroperm 500F and supermendur ferromagnetic cores used in a linear generator for oceanic wave energy conversion," in *Proc. Int. Conf. Robot., Elect. Signal Process. Techn. (ICREST)*, Shanghai, China, Jan. 2019, pp. 602–605.
[34] S. Molla, O. Farrok, K. M. Muttaqi, and M. R. Islam, "Design of a direct drive linear generator with high flux density magnetic cores for oceanic wave energy conversion," in *Proc. IEEE Int. Conf. Appl. Supercond. Electromagn. Devices (ASEMD)*, Tianjin, China, Apr. 2018, pp. 1–2.
[35] S. Molla and O. Farrok, "Use of high flux density ferromagnetic cores in linear generators for oceanic wave energy conversion," in *Proc. Int. Conf. Electr., Comput. Commun. Eng. (ECCE)*, Feb. 2019, pp. 1–5.
[36] O. Farrok, M. Rahman Kiran, M. Rabiul Islam, W. Xu, and J. Zhu, "Core loss minimization of the linear generator by using high graded magnetic materials for harvesting oceanic wave energy," in *Proc. IEEE Int. Electr. Mach. Drives Conf. (IEMDC)*, San Diego, CA, USA, May 2019, pp. 1762–1765.
[37] A. Dahir Tahlil, O. Farrok, and K. Ahmed, "XFlux material based permanent magnet linear electrical generator connected to a single piston hydraulic free piston engine," in *Proc. IEEE Int. Conf. Power, Electr., Electron. Ind. Appl. (PEEIACON)*, Dhaka, Bangladesh, Nov. 2019, pp. 118–121.
[38] R. Vermaak and M. J. Kamper, "Design aspects of a novel topology air-cored permanent magnet linear generator for direct drive wave energy converters," *IEEE Trans. Ind. Electron.*, vol. 59, no. 5, pp. 2104–2115, May 2012.
[39] N. P. Gargov and A. F. Zobaa, "Multi-phase air-cored tubular permanent magnet linear generator for wave energy converters," *IET Renew. Power Gener.*, vol. 6, no. 3, pp. 171–176, May 2012.
[40] R. Vermaak and M. J. Kamper, "Experimental evaluation and predictive control of an air-cored linear generator for direct-drive wave energy converters," *IEEE Trans. Ind. Appl.*, vol. 48, no. 6, pp. 1817–1826, Nov. 2012.
[41] I. Stamenkovic, N. Milivojevic, N. Schofield, M. Krishnamurthy, and A. Emadi, "Design, analysis, and optimization of ironless stator permanent magnet machines," *IEEE Trans. Power Electron.*, vol. 28, no. 5, pp. 2527–2538, May 2013.
[42] J. R. Burns, "Ocean wave energy conversion using piezoelectric material members," U.S. Patent 4 685 296, Aug. 11, 1987.
[43] M. Daniel, C. Montserrat, P. David, M. Antoni, and M. Jaume, "An impacting energy harvester through piezoelectric device for oscillating water flow," in *Proc 5th MARTECH Int. Workshop Mar. Technol.*, Girona, Spain, 2013, pp. 39–42.
[44] N. V. Viet, X. D. Xie, K. M. Liew, N. Banthia, and Q. Wang, "Energy harvesting from ocean waves by a floating energy harvester," *Energy*, vol. 112, pp. 1219–1226, Oct. 2016.
[45] C. Viñolo, D. Toma, A. Mànuel, and J. del Rio, "An ocean kinetic energy converter for low-power applications using piezoelectric disk elements," *Eur. Phys. J. Special Topics*, vol. 222, no. 7, pp. 1685–1698, Sep. 2013.
[46] G. A. Athanassoulis and K. I. Mamis, "Modeling and analysis of a cliff-mounted piezoelectric sea-wave energy absorption system," *Coupled Syst. Mech.*, vol. 2, no. 1, pp. 53–83, Mar. 2013.
[47] H. Mutsuda, R. Watanabe, M. Hirata, Y. Doi, and Y. Tanaka, "Elastic floating unit with piezoelectric device for harvesting ocean wave energy," in *Proc. Ocean Space Utilization; Ocean Renew. Energy*, vol. 7. Rio de Janeiro, Brazil, Jul. 2012, pp. 233–240.
[48] F.-R. Fan, Z.-Q. Tian, and Z. Lin Wang, "Flexible triboelectric generator," *Nano Energy*, vol. 1, no. 2, pp. 328–334, Mar. 2012.
[49] Y. Xie, S. Wang, S. Niu, L. Lin, Q. Jing, J. Yang, Z. Wu, and Z. L. Wang, "Grating-structured freestanding triboelectric-layer nanogenerator for harvesting mechanical energy at 85% total conversion efficiency," *Adv. Mater.*, vol. 26, no. 38, pp. 6599–6607, Oct. 2014.
[50] G. Zhu, Y. Zhou, P. Bai, X. Meng, Q. Jing, J. Chen, and Z. Wang, "A shape-adaptive thin-film-based approach for 50% high-efficiency energy generation through micro-grating sliding electrification," *Adv. Mater.*, vol. 26, no. 23, pp. 3788–3796, Jun. 2014.
[51] A. R. M. Foisal and G.-S. Chung, "Fabrication and characterization of a low frequency electromagnetic energy harvester," *J. Semicond.*, vol. 33, no. 7, Jul. 2012, Art. no. 074001.
[52] X. Wang, S. Niu, Y. Yin, F. Yi, Z. You, and Z. L. Wang, "Triboelectric nanogenerator based on fully enclosed rolling spherical structure for harvesting low-frequency water wave energy," *Adv. Energy Mater.*, vol. 5, no. 24, Nov. 2015, Art. no. 1501467.
[53] A. Ahmed, Z. Saadatnia, I. Hassan, Y. Zi, Y. Xi, X. He, J. Zu, and Z. L. Wang, "Self-powered wireless sensor node enabled by a duck-shaped triboelectric nanogenerator for harvesting water wave energy," *Adv. Energy Mater.*, vol. 7, no. 7, Apr. 2017, Art. no. 1601705.
[54] Z.-H. Lin, G. Cheng, W. Wu, K. C. Pradel, and Z. L. Wang, "Dual-mode triboelectric nanogenerator for harvesting water energy and as a self-powered ethanol nanosensor," *ACS Nano*, vol. 8, no. 6, pp. 6440–6448, May 2014.
[55] T. Jiang, H. Pang, J. An, P. Lu, Y. Feng, X. Liang, W. Zhong, and Z. L. Wang, "Robust swing-structured triboelectric nanogenerator for efficient blue energy harvesting," *Adv. Energy Mater.*, vol. 10, no. 23, 2020, Art. no. 2000064.
[56] X. Liang, T. Jiang, G. Liu, Y. Feng, C. Zhang, and Z. L. Wang, "Spherical triboelectric nanogenerator integrated with power management module for harvesting multidirectional water wave energy," *Energy Environ. Sci.*, vol. 13, no. 1, pp. 277–285, Jan. 2020.

[57] J. Chen, J. Yang, Z. Li, X. Fan, Y. Zi, Q. Jing, H. Guo, Z. Wen, K. C. Pradel, S. Niu, and Z. L. Wang, "Networks of triboelectric nanogenerators for harvesting water wave energy: A potential approach toward blue energy," *ACS Nano*, vol. 9, no. 3, pp. 3324–3331, Feb. 2015.
[58] L. Xu, T. Jiang, P. Lin, J. J. Shao, C. He, W. Zhong, X. Y. Chen, and Z. L. Wang, "Coupled triboelectric nanogenerator networks for efficient water wave energy harvesting," *ACS Nano*, vol. 12, no. 2, pp. 1849–1858, Jan. 2018.
[59] Z. L. Wang, T. Jiang, and L. Xu, "Toward the blue energy dream by triboelectric nanogenerator networks," *Nano Energy*, vol. 39, pp. 9–23, Sep. 2017.
[60] M. R. Islam and M. R. I. Sheikh, "Fuzzy logic based an improved controller for wave energy conversion systems," in *Proc. Int. Conf. Electr. Eng. Inf. Commun. Technol. (ICEEICT)*, Dhaka, Bangladesh, May 2015, pp. 1–6.
[61] O. Farrok, M. R. I. Sheikh, and M. R. Islam, "An advanced controller to improve the power quality of microgrid connected converter," in *Proc. Int. Conf. Electr. Electron. Eng. (ICEEE)*, Nov. 2015, pp. 185–188.
[62] H. Jing, N. Maki, T. Ida, and M. Izumi, "Performance comparison of MW class tubular linear generators for wave energy conversion," *IEEE Trans. Appl. Supercond.*, vol. 27, no. 6, pp. 1–6, Sep. 2017.
[63] H. Mutsuda, K. Kawakami, M. Hirata, Y. Doi, and Y. Tanaka, "Study on wave power generator using flexible piezoelectric device," in *Proc. Ocean Space Utilization; Ocean Renew. Energy*, vol. 5. Rotterdam, The Netherlands, Jan. 2011, pp. 267–273.

ABIDUR RAHMAN received the B.Sc. and M.Sc. degrees in electrical and electronic engineering (EEE) from the Ahsanullah University of Science and Technology (AUST), Dhaka, Bangladesh, in 2016 and 2020, respectively.

He was a Lecturer with Northern University, Dhaka, from 2016 to 2018. He has been a Lecturer with the Department of EEE, AUST, since 2019. His research interests include smart grid, renewable energy sources, and electric machines. He received the Dean's List of Honor for academic excellence.

OMAR FARROK (Member, IEEE) received the Ph.D. degree from the Department of Electrical and Electronic Engineering (EEE), Rajshahi University of Engineering and Technology (RUET), Rajshahi, Bangladesh, in 2016.

He has been a Distinct Associate Professor with the Department of EEE, Ahsanullah University of Science and Technology (AUST), Dhaka, Bangladesh, since 2016. He has authored or coauthored more than 60 technical articles, including ten the IEEE TRANSACTIONS/Journal articles in international journals and conference proceedings. His research interests include oceanic wave energy converter, linear electrical generator, magnetic material, electrical machine and drive, renewable energy systems, electromagnetics, and power electronics.

Dr. Farrok is a Life Fellow of the Institution of Engineers, Bangladesh (IEB). He was registered with the Board of Bangladesh Professional Engineers Registration Board (BPERB), as a Professional Engineer (P.Eng.), in 2017. He received the Four Best Paper Awards from the IEEE ICEMS, Sydney, NSW, Australia, in 2017, ASEMD, Tianjin, China, in 2018, ICEMS, Harbin, China, in 2019, and PEEIACON, Dhaka, Bangladesh, in 2019. He is elected as the chair, co-chair, and nominated as a member of several technical committees formed by the Bangladesh Government under the Ministry of Industries and others.

MD. RABIUL ISLAM (Senior Member, IEEE) received the Ph.D. degree in electrical engineering from the University of Technology Sydney (UTS), Sydney, NSW, Australia, in 2014.

He was a Lecturer with RUET, in 2005, and a Full Professor, in 2017. In 2018, he joined the School of Electrical, Computer, and Telecommunications Engineering (SECTE), University of Wollongong (UOW), Wollongong, NSW, Australia. He has authored or coauthored 160 articles, including 45 the IEEE TRANSACTIONS/IEEE Journal articles in international journals and conference proceedings. He has written or edited four technical books published by Springer. He received several funding from the Government and Industries, including the Australian Government ARC Discovery Project 2020 entitled, A Next Generation Smart Solid-State Transformer for Power Grid Applications?. His research interests include power electronic converters, renewable energy technologies, power quality, electrical machines, electric vehicles, and smart grid.

Dr. Islam serves as an Editor for the IEEE TRANSACTIONS ON ENERGY CONVERSION and the IEEE POWER ENGINEERING LETTERS. He also serves as an Associate Editor for IEEE ACCESS. He served as a Guest Editor for the IEEE TRANSACTIONS ON ENERGY CONVERSION, the IEEE TRANSACTIONS ON APPLIED SUPERCONDUCTIVITY, and *IET Electric Power Applications*.

WEI XU (Senior Member, IEEE) received the B.E. and M.E. degrees in electrical engineering from Tianjin University, Tianjin, China, in 2002 and 2005, respectively, and the Ph.D. degree in electrical engineering from the Institute of Electrical Engineering, Chinese Academy of Sciences, in 2008.

From 2008 to 2012, he was a Postdoctoral Fellow with the University of Technology Sydney, a Vice Chancellor Research Fellow with the Royal Melbourne Institute of Technology, and a Japan Science Promotion Society Invitation Fellow with Meiji University. Since 2013, he has been a Full Professor with the State Key Laboratory of Advanced Electromagnetic Engineering, Huazhong University of Science and Technology, China. He has more than 100 articles accepted or published with the IEEE TRANSACTIONS JOURNALS, two edited books published by Springer Press, and one monograph published by China Machine Press. He holds over 120 invention patents granted or pending in electrical machines and drives. His research interests include design and control of linear/rotary machines.

Dr. Xu is a Fellow of the Institute of Engineering and Technology (IET). He will serve as the General Chair for the International Symposium on Linear Drives for Industry Applications (LDIA) and the IEEE International Conference on Predictive Control of Electrical Drives and Power Electronics (PRECEDE), Wuhan, China. He served as an Associate Editor for the several IEEE TRANSACTIONS JOURNALS, such as the IEEE TRANSACTIONS ON INDUSTRIAL ELECTRONICS and so on.